PhD degree in Molecular Medicine (curriculum in Molecular Oncology)

European School of Molecular Medicine (SEMM),

University of Milan and University of Naples "Federico II"

Settore disciplinare: MED/04

The adhesion molecule L1: a novel player in ovarian cancer vasculature

Francesca Angiolini

IEO, Milan

Matricola n. R10331

Supervisor:

Dr. Ugo Cavallaro

IEO, Milan

Added Supervisor:

Prof. Salvatore Pece

IEO, Milan

Anno accademico 2015-2016

TABLE OF CONTENTS

LIST OF ABBREVIATIONS

ACTB	beta-actin
ADAMs	disintegrin and metalloproteinases
ALDH	aldehyde dehydrogenase
ANGS	angiopoietins
BM	basement membrane
BMDCs	bone marrow-derived cells
BSA	bovine serum albumin
CDH2	cadherin-2
CM	conditioned medium
CSCs	cancer stem cells
CT	carboplatin/paclitaxel
DFS	disease free survival
DMSO	dimethyl sulfoxide
DNA	deoxyribonucleic acid
ECGS	endothelial cell growth supplement
ECs	endothelial cells
EDTA	Ethylenediaminetetraacetic acid
EGR1	early growth response protein 1
EMT	epithelial–mesenchymal transition
EMT-TFs	epithelial–mesenchymal transition inducing transcriptional factors
EOC	ephitelial ovarian cancer
FACS-sorting	fluorescence-activated cell sorting
FBS	fetal bovine serum
FDA	food and drug administration
FGF	fibroblast growth factor

FGFR	fibroblast growth factor receptor
FNIII-like	fibronectin type III repeats
GAPDH	glyceraldehyde-3-phosphate dehydrogenase
GFP	green fluorescent protein
H&E	hematoxylin and eosin
IL-6	interleukin 6
Klf4	kruppel-like factor 4
Krt8	keratin 8
L1-ICD	L1 intracellular domain
L1CAM	L1 Cell Adhesion Molecule
luECs	lung-derived endothelial cells
OC	ovarian cancer
OCSCs	ovarian cancer stem cells
OS	overall survival
OSE	ovarian surface epithelium
PBS	phosphate buffered saline
PDGF	platelet derived growth factor
PFA	paraformaldehyde
PlGF	placental growth factor
PSF	progression free survival
qRT-PCR	quantitative reverse transcriptase polymerase chain reaction
RNA	ribonucleic acid
Robo4	roundabout Guidance Receptor 4
RT	room temperature
RTKs	receptor tyrosine kinases
SDS	sodium Dodecyl Sulphate
SDS-PAGE	sodium Dodecyl Sulphate - PolyAcrylamide Gel Electrophoresis

SEM	scanning Electron Microscopic
SFE	sphere forming efficiency
shRNA	short hairpin RNA
Sipa 1	signal-induced proliferation-associated protein 1
Snail1	Snail Family Zinc Finger 1
Snail2	Snail Family Zinc Finger 2
TBS	tris-buffered saline
TGFbeta	transforming growth factor-beta
TIC	tubal intraepithelial carcinoma
TKIs	tyrosine kinase inhibitors
VE-cadherin	vascular endothelial cadherin
VEGF	vascular endothelial growth factor receptor
VEGFR	vascular endothelial growth factor receptor
Vim	vimentin
Zeb1	zinc Finger E-Box Binding Homeobox 1
Zeb2	zinc Finger E-Box Binding Homeobox 2

FIGURE INDEX

LIST OF TABLES

ABSTRACT

Ovarian cancer represents an outstanding clinical challenge because of its high mortality rate, mainly due to tumor relapse and chemoresistance. The identification of novel targets and strategies for the treatment of OC is clearly an unmet need in clinical oncology. In this context, drugs that interfere with tumor neovascularization have shown promising results in recent clinical trials. However, the beneficial effect of anti-angiogenic therapies is often modest and transient: in OC patients, for example, it has been observed only a limited increase in progression-free survival.

Thus, the definition of novel druggable targets within the tumor vasculature will have profound implications, particularly for those tumor types, such as OC, that respond poorly to conventional anti-cancer treatments.

L1 is a transmembrane glycoprotein belonging to the immunoglobulin superfamily that was initially characterized as an adhesion molecule playing a key role in the development of nervous system. However, several studies have demonstrated its involvement in several types of human cancer, including ovarian carcinoma. In this context, L1 expression is generally associated with poor diagnosis, an aggressive behavior and advanced tumor stage. Moreover, L1 induces a motile and invasive phenotype, supporting metastatic spread, and promotes chemoresistance.

Our laboratory has obtained compelling evidence that L1 is aberrantly expressed in tumor vasculature and exerts an unexpected, pleiotropic function in endothelial cells.

Based on these findings and on the pivotal role of angiogenesis in ovarian cancer, in this work I have investigate the functional role of L1 within the OC-associated vasculature. My results revealed that L1 is particularly abundant in OC vasculature as compared to normal vessels. Moreover,, vascular L1 was found to be a causal player in OC progression, possibly due to an endothelial cell-autonomous effect on OC vascularization, concomitant

to a positive regulation of ovarian cancer stem cell function.

This research, besides giving insights into novel pathways involved in pathological angiogenesis, provides the rationale for exploring the clinical relevance of L1 expression and function in OC vessels and in their crosstalk with tumor cells, possibly opening new avenues for the development of innovative targeted therapies for OC malignancy.

1. INTRODUCTION

1.1 Tumor Angiogenesis

During embryonic development new vessels form by assembly of endothelial precursors, called angioblasts, which are able to organize a primitive vascular network of small capillaries. This process is called vasculogenesis [1]. Then, vessel sprouting underlies the initial phases of angiogenesis (from the greek *angêion*, vessels, e *genesis*, birth), which is the formation of new vessels from preexisting blood vessels by proliferation and migration of endothelial cells (ECs) in response to a proangiogenic stimulus. This creates a more organized vasculature architecture that remodels into arteries and veins [2] (Figure. 1).

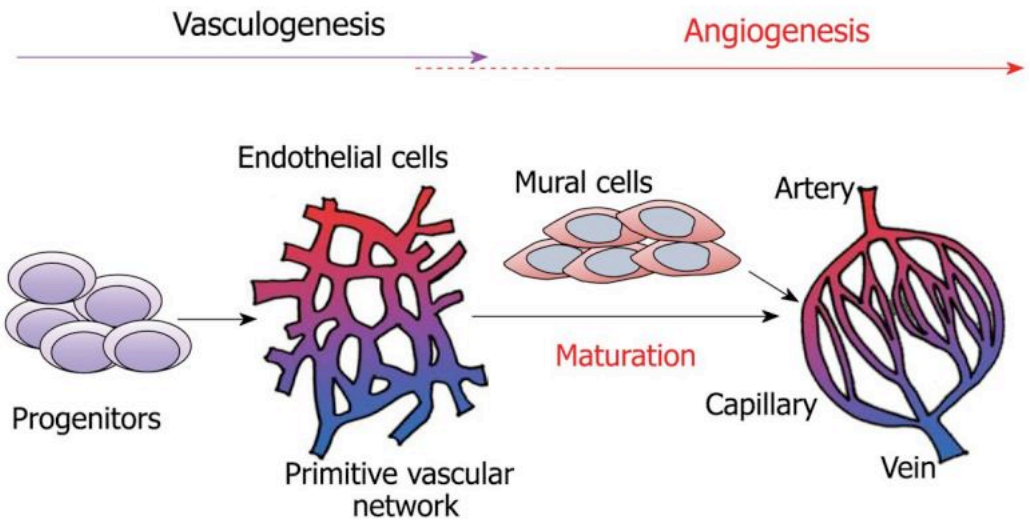

Figure 1. ***Schematic representation of vessel formation.***
During embryonic development new vessels form by the assembly of endothelial progenitors through vasculogenesis. Later, angiogenesis determines the formation of additional vessels by proliferation of preexisting ECs. The vascular network is stabilized by the recruitment of mural cells (Adapted from Yoh Takuwa et al. 2010, [3]).

Subsequently, the newly formed vessels are stabilized by the recruitment of pericytes and

vascular smooth muscle cells that enwrap nascent EC tubules [4] and by generating extracellular matrix. Collectively these processes result in the maturation and stabilization of the vessels.

In the adult, vessels are quiescent and rarely form new branches. However, ECs maintain their plasticity and their ability to respond to angiogenic signals both in physiological situations, such as wound healing, in the cycling ovary or in the placenta during pregnancy, but also in pathological conditions such as inflammatory disorders and cancer [5].

In 1971, Judah Folkman first formulated the hypothesis that tumor growth depends on angiogenesis [6]. Indeed, solid tumors can grow beyond a certain size (~2 mm) only if they induce the formation of new blood vessels that supply oxygen and nutrients to cancer cells. During tumorigenesis, EC may be re-activated from a resting to a proliferative state by several signals, which can be produced by tumor, stromal or immune cells or can be mobilized from the extracellular matrix [7]. This "angiogenic switch" strictly depends on an increased production of pro-angiogenic factors, such as vascular endothelial growth factor (VEGF), fibroblast growth factor-2 (FGF-2), placental growth factor (PlGF), transforming growth factor-beta (TGFbeta), platelet derived growth factor (PDGF) and angiopoietins (Angs). Moreover, this switch may also involve the down-regulation of anti-angiogenic modulators such as endostatin. Overall, the imbalance of angiogenic regulators in favor of pro-angiogenic stimuli determines the establishment of an "angiogenic state" that results in the formation of a chaotic vascular architecture (Figure. 2). The newly formed blood vessel network provides tumors with oxygen and nutrients, thus allowing the cancer cells to proliferate and form metastases. Indeed, tumor vessels offer a critical route for cancer dissemination to distant organs [8].

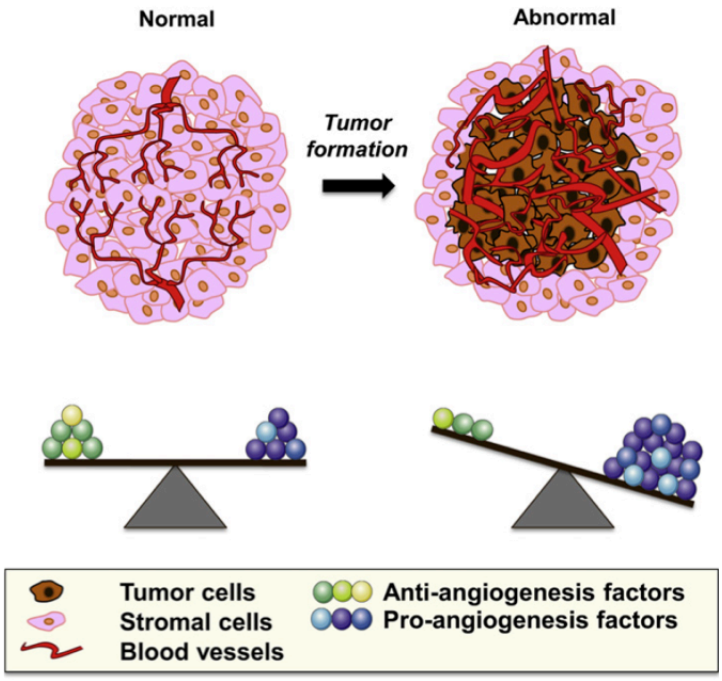

Figure 2. ***An imbalance between anti- and pro-angiogenic factors resulted in uncontrolled neo- vascularization in tumor.***

In normal tissues ECs are usually quiescent and the action of pro-angiogenic factors is balanced by the effects of anti-angiogenic molecules. Conversely, in tumors an uncontrolled production of pro-angiogenic factors determines the reactivation of ECs which results in the formation of a chaotic vessel network that in turn foster tumor cell proliferation (adapted from Sandy Giuliano & Gilles Pagès 2013, [9]).

In normal tissues, mature ECs are connected by intercellular junctions that are able to stabilize the vessel wall [10]. In addition, perivascular cells, including both pericytes and vascular smooth muscle cells, firmly interact with ECs to stabilize vessels. Conversely, the vasculature associated to tumors is structurally abnormal. Indeed, tumor vessels are highly disorganized, tortuous, dilated and heterogeneous in size [11]. The ECs lining tumor vessel possess an irregular morphology (Figure. 3). Tumor ECs are abnormal in shape, they grow on top of each other and project into the lumen. Moreover, vascular endothelium in tumors is often leaky, with ECs loosely attached one to the other, and contains several fenestrations, resulting in hemorrhage and increased interstitial fluid pressure [12] (Figure.

4). These defects, together with poor pericyte coverage and an absent/irregular basement membrane deposition, contribute to vascular instability and altered permeability [12,13]. Consequently, tumor blood flow is chaotic and irregular within the mass. The abnormal tumor vasculature favours a tumor microenvironment characterized by an impaired tumor oxygenation that, in turn, leads to hypoxia-induced tumor growth and dissemination while diminishing the response to therapy and radiation [14]. As a matter of fact, the development of drugs able to interfere with tumor vessel abnormalities or to block/inactivate the function of pro-angiogenic molecules is being actively pursued as a promising therapeutic strategy in oncology.

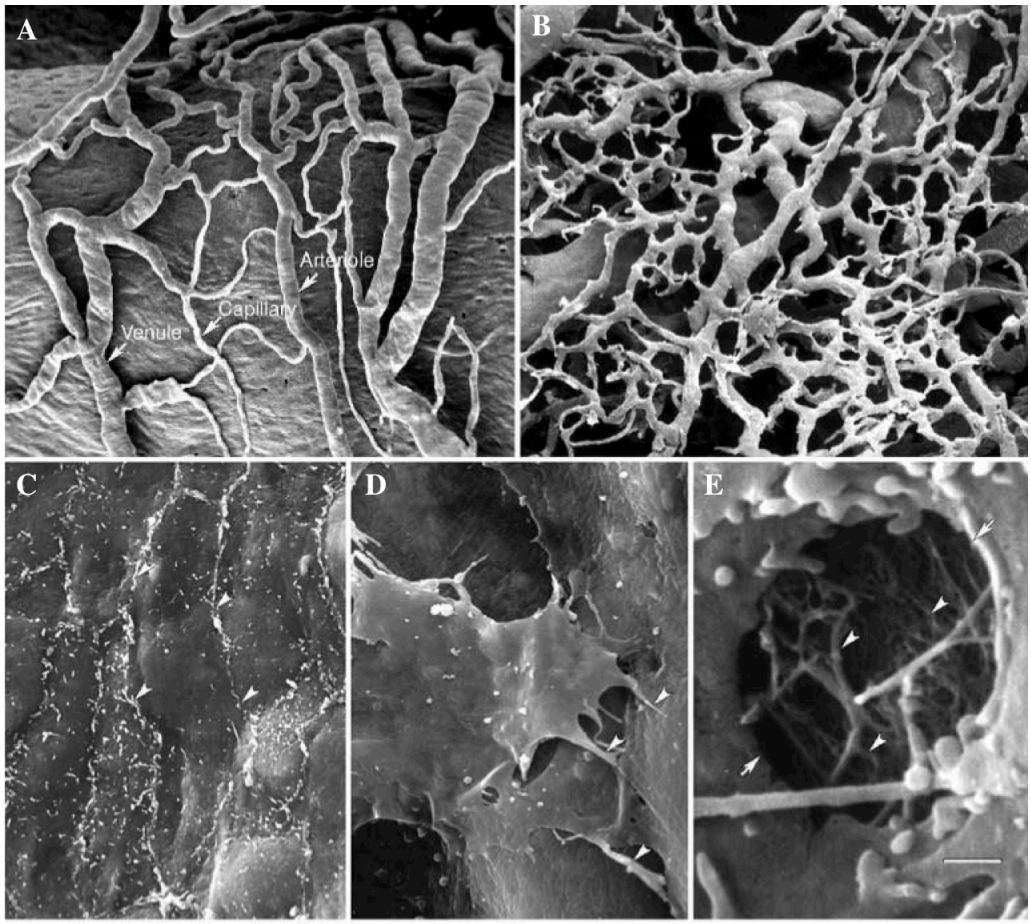

Figure 3. ***Scanning Electron Microscopic (SEM) imaging of normal and tumor vessels.*** *(A) SEM imaging of normal microvasculature showing arterioles, capillaries and venules gerarchically organized. (B) SEM imaging of tumor microvasculature characterized by chaotic organization and the lack of conventional hierarchy of blood vessels. (C) SEM imaging of the luminal surface of normal vessel. EC are tightly attached on to the other*

(arrowed). (D-E) SEM imaging of the luminal surface of tumor vessel. Interendothelial contacts are weakened (arrowed), EC protrude into the lumen and contain several fenestrations (E) (Adapted from M McDonald & Peter L Choyke 2003, [15])

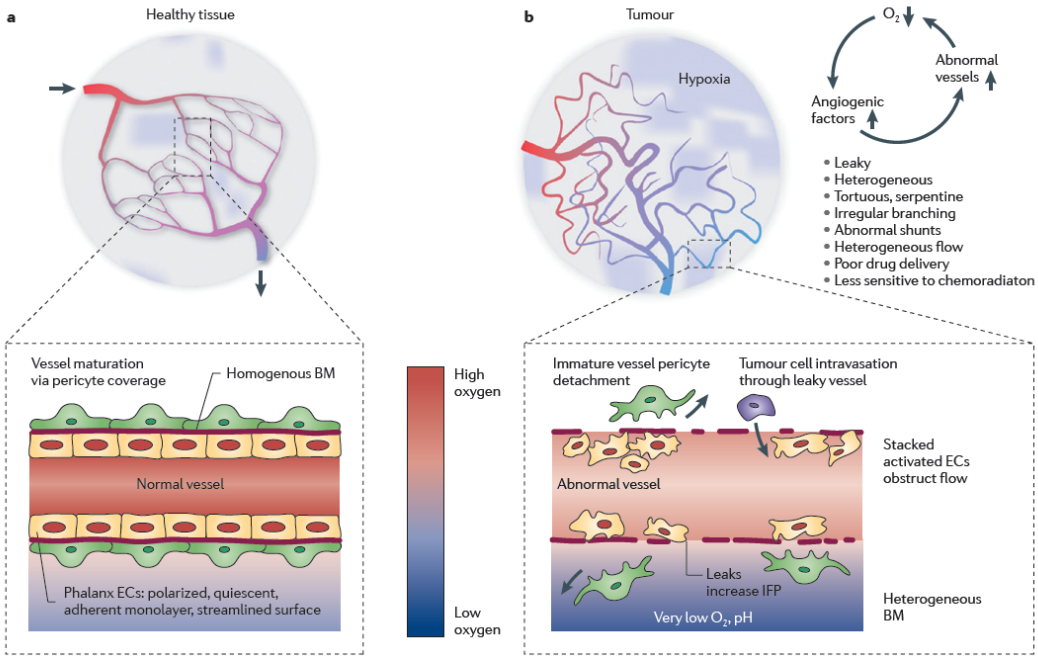

Figure 4. ***Tumor vessels are functionally abnormal.***

(A) In healty tissues vessels are lined by ECs (in yellow) that relay on basement membrane (BM, in red) and they are stabilized by perycites (in green). (B)In tumors, ECs are loosely attached one to the other, BM is discontinuous and pericytes detached from BM. Collectively, these abnormal features establish an irregular and heterogeneous blood flow in tumor mass and determin an increase of interstitial fluid pressure (Adapted from Peter Carmeliet & Rakesh K. Jain 2011, [11]).

1. 1. 2 VEGF-based anti-angiogenic therapy in cancer

The pathophysiological changes affecting tumor vasculature described in paragraph 1. 1 have several implications on tumor behavior. On one hand, hypoxic tumor cells usually have a more aggressive phenotype and they are more prone to metastasize. On the other hand, the abnormal blood flow and the irregular distribution of vessels, together with the

increased vascular permeability, could also prevent the delivery of systemically administered cytotoxics to all areas of the tumor mass.

The revolutionary concept of treating tumor by inhibiting new blood vessel formation was established by Judah Folkman in 1971 [6]. Indeed, since most tumors cannot grow without a blood supply, the general idea was to find ways to block tumor neo-vascularization in order to starve it, thus preventing its growth and the development of metastases.

Research in tumor angiogenesis and anti-angiogenic compounds progressed slowly until the discovery of a major angiogenic driver, the vascular endothelial growth factor (VEGF) [16,17]. Over the last decades many investigators have embarked on the design of therapeutic strategies that, by interfering with the angiogenic cascade, would prevent cancer growth and metastasis [18]. The most prominent output of these efforts has been the approval for the clinical use of drugs that inhibit the VEGF pathway. The first compound that has been approved by FDA in 2004 for clinical purposes was Bevacizumab (Avastin, Genentech), a humanized monoclonal antibody targeting VEGF. Thereafter, several small-molecule tyrosine kinase inhibitors (TKIs) of VEGFRs have been developed and some of them are currently under clinical investigation, such as cediranib [19] and pazopanib [20].

Early preclinical studies corroborated the hypothesis that inhibiting blood vessels starve tumors to death or render them dormant. In 1993, Napoleone Ferrara reported that the treatment with anti-VEGF monoclonal antibody of mice bearing xenografts of glioblastoma multiforme, leiomyosarcoma or rhabdomyosarcoma caused a decrease in vessel density and a significant reduction of tumor growth [21]. These results were also confirmed by the same group in a mouse model of colorectal cancer [22].

Despite the exciting and promising results obtained in preclinical models, the use of anti-VEGF drugs as monotherapy in clinical setting showed modest benefit in terms of survival [23]. However, the combination of VEGF blockade by Bevacizumab with standard chemotherapy in phase III trials has yielded improved OS or PFS in metastatic colorectal and non-small cell lung cancer patients, thus supporting the rationale of targeting tumor

vasculature to improve the efficacy of cytostatic agents [24-28]. Since the anti-angiogenic therapy aims at reducing blood vessel, this might hamper the efficacy of systemically administered chemotherapy, which in fact relies on efficient tumor blood flow. These observations might seem in contrast with the improved progression free survival (PFS) and overall survival (OS) obtained in clinic by the combination of Bevacizumab with the chemotherapy. This apparent "paradox" might be solved by the provocative paradigm of "*vascular normalization"* postulated by Rakesh Jain in 2001 [14]. He proposed to restore the balance between pro- and anti-angiogenic signals back toward a quiescent state by a judicious use of anti-angiogenic agents (Figure. 5), mainly represented by anti-VEGF drugs. Rather than destroying newly formed tumor vessels, anti-angiogenic therapy should take vessel structure and function back to a "normal-like" state.

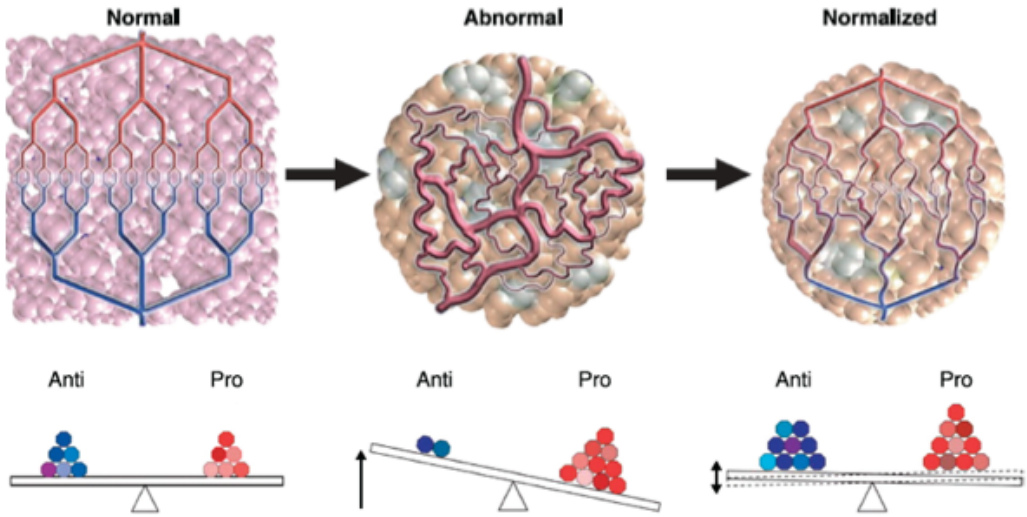

Figure 5. ***Vascular normalization.***

The tumor-associated vasculature is functionally and structurally abnormal. The treatment of tumor with an anti-angiogenic drug might revert tumor vessel abnormalities to a more normal phenotype reestablishing the balance between pro-angiogenic and anti-angiogenic factors (Adapted from Shom Goel et al. 2011, [29]).

A large number of preclinical studies confirmed the existence of a normalized vessel phenotype upon anti-VEGF treatment [30,31]. They revealed a reduction in vessel density, increased pericyte coverage, improved tumor oxygenation and reduced vascular permeability. These reports demonstrated also the existence of a "normalization window", namely a time interval, usually within the first three days of treatment, that begins with the appearance of a normalized vasculature and ends with the disappearance of its hallmarks.

These promising results demonstrating a synergism between anti-VEGF therapy and chemotherapy in preclinical models, have fostered a number of clinical studies in human to verify whether vascular normalization occurs also in patients [32,33]. Even if these studies are complex and they have several limits, such as the inability to perform several biopsies and at scheduled time points on the same patient, they have provided evidence of vascular normalization [34].

Unfortunately, vascular normalization is a transient phenomenon and the benefits resulting from the addition of anti-angiogenic therapy to standard chemotherapy are only temporary. In fact, early after the beginning of the anti-angiogenic treatment, tumors develop resistance to VEGF therapy and become able to overcome the blockade of angiogenic pathways.

1. 1. 3 Possible modes of resistance to anti-angiogenic drugs

Despite promising results were obtained in preclinical models, the inhibitors of VEGF and of its receptor (VEGFR) displayed only partial beneficial effects on certain solid tumors and in many cases cancers develop resistance/escape mechanisms or are refractory to VEGF blockade [35]. A still evolving and not yet definitive hypothesis is that the angiogenic tumor adapt to the drug and it can elude the blockade of angiogenesis in several ways [36] (Figure. 6):

- activating alternative pro-angiogenic pathways, such as FGF/FGFR signaling, thus compensating for the VEGF-blockade (Figure . 6A);

- recruiting endothelial/stromal precursors from bone marrow (bone marrow-derived cells, BMDCs) that can fuel tumor growth and the angiogenic process in a VEGF-independent way (Figure. 6B);
- increasing the pericyte coverage of tumor vessels. The recruitment of these cells help vessels in protecting them from death caused by the anti-angiogenic treatment (Figure. 6C);
- selecting clones with a more aggressive behavior and with a higher metastatic potential. These clones will be more prone to colonize to normal tissues and form distal metastasis to escape oxygen and nutrient deprivation (Figure. 6D).

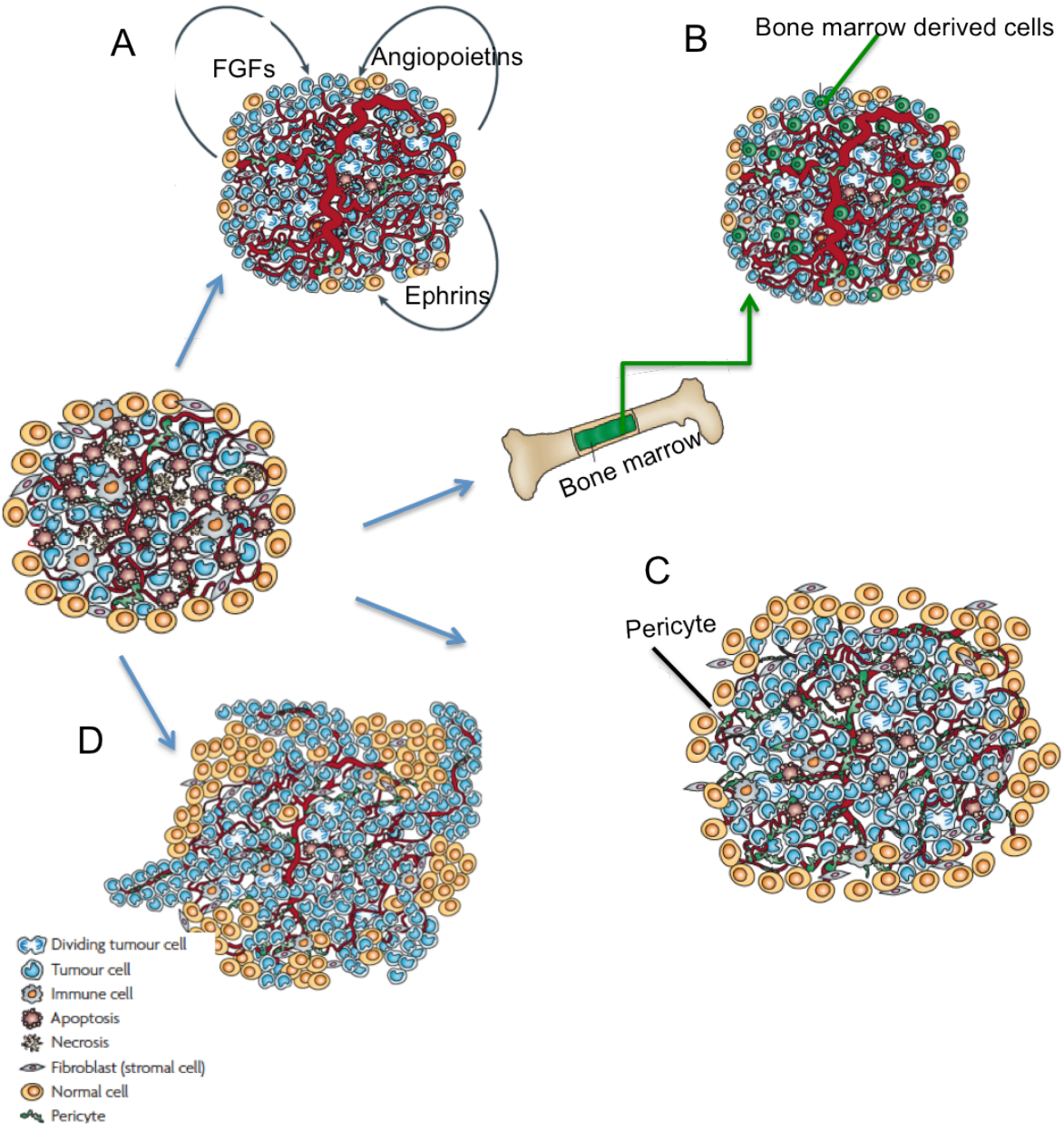

Figure 6. ***Possible modes of resistance to VEGF-based anti-angiogenic drugs.***
Shortly after the beginning of the treatment with an anti-VEGF drug, tumors may acquire resistance to therapy. (A) Tumor cells activate alternative pro-angiogenic pathways that compensate for the depletion of VEGF. (B) Tumor recruits endothelial cells from bone marrow. (C) Tumor vessels increase their pericyte coverage avoiding the death caused by the anti-angiogenic drug. (D) Tumor cells with high invasive and metastatic potential are selected, which are able to migrate and colonize other normal tissues (adapted from Gabriel Bergers & Douglas Hanahan 2008, [36]*).*

A deeper understanding of the modes of resistance to VEGF-based therapy and the underling mechanisms will offer the essential opportunity to improve the benefits of anti-

angiogenic therapy and to overcame the current limits of such treatments.

1. 1. 4 Current limits of anti-angiogenic drugs and future directions

In addition to the development of resistance/escape mechanisms, the discordance between preclinical and clinical studies with regard to the outcome of anti-angiogenic treatments can be explained comparing more closely the studies themselves [37]:

1. the preclinical tumor models employed grow rapidly and are more sensitive to anti-VEGF agents than their human counterparts;
2. anti-angiogenic therapy was usually used to treat primary tumor in preclinical models while almost all anti-angiogenic agents had been approved for metastatic diseases in clinic;
3. while most preclinical studies used these drugs as monotherapies, several anti-angiogenic compounds showed improved OS only when combined with chemo- or immune-therapeutics;
4. the dose of anti-angiogenic drug utilized in many preclinical studies has been incompatible with clinical purposes, possibly leading to misleading results.

In order to obtain results that can be easily transfered into clinic, a more appropriate experimental design and preclinical data interpretation is needed.

In addition, several strategies may help in overcoming the limitations of current anti-angiogenic treatments. The first aspect to take into account is that a tumor must be considered as an organ. Beside tumor cells, it consists of several other cell types, including endothelial cells, pericytes, immune cells and fibroblasts, that together form a tumor microenvironment able to promote tumor cell proliferation, metastasis and resistance to various therapies. Moreover, current antitumor and vascular normalization therapies have mainly focused on endothelial cell-dependent angiogenesis, overlooking several other mechanisms of neovascularization. It is clear now that tumor vasculature is not necessarily dependent of endothelial cell proliferation and sprouting of new capillaries [38]. Beside ECs,

other cell types actively participate at the formation of tumor vasculature, including stem cells, cancer stem cells, BM-derived endothelial progenitors through at least four ways [38,39]:

1. intussusceptive angiogenesis, where preexisting vessel divided into two new blood vessels by the formation of transvascular pillar inside vessel lumen.
2. blood vessel co-option, in which tumor cells grow along already existing vessel without inducing the formation of new capillaries;
3. vasculogenic mimicry, where tumor cells dedifferentiate into endothelial-like cells and start forming tube structures;
4. mobilizing bone marrow-derived circulating endothelial progenitor cells, which are able to assemble into newly blood vessels.

Thus, the concomitant targeting of tumor cells, bone marrow-derived cells, and other vasculogenic cells in a tumor microenvironment, as well as targeting more than one angiogenic-related pathways at the same time, may improve the efficacy of anti-angiogenic therapy, possibly improving also the benefits of vascular normalization (Figure. 7).

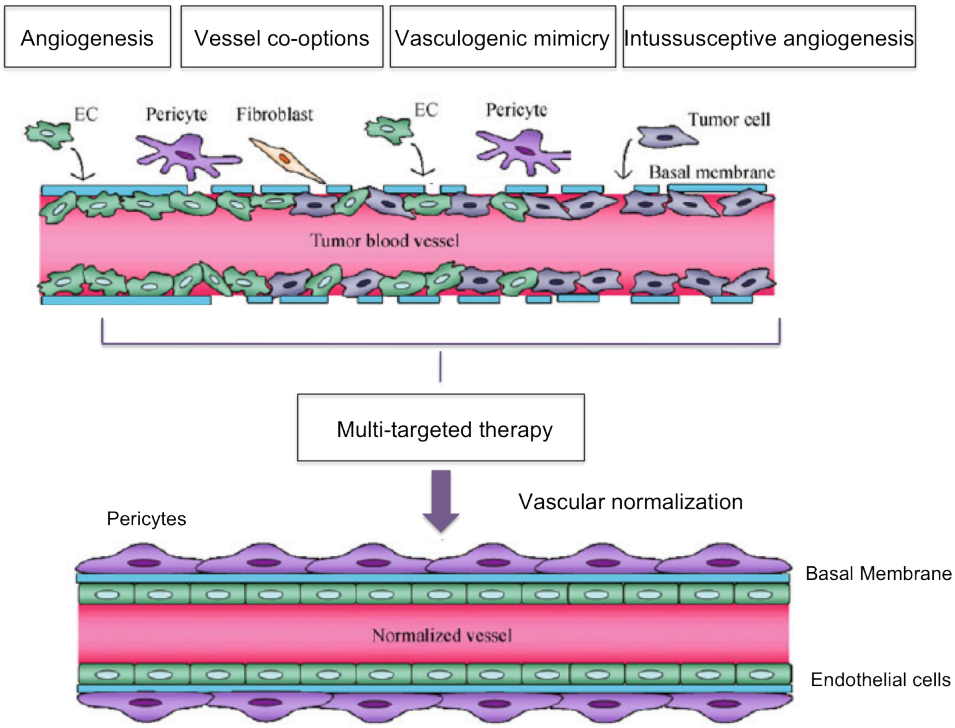

Figure 7. ***Mechanisms of neovascularization.***

Tumors vessels form by several mechanisms including sprouting angiogenesis, vessel co-option between tumor and endothelial cells, vasculogenic mimicry and intussusceptive angiogenesis. In these processes not only ECs are involved but also several other cell types such as pericytes, bone-marrow derived cells and tumor cells. A novel therapeutic approach able to hit several targets and different cell types concomitantly might increase the benefit of current anti-angiogenic therapy and vascular normalization (Adapted from Bingxue Shang et al. 2012, [40]).

Finally, new targets should be identified, an objective that can only be achieved through a deeper understanding of the molecular players and mechanisms that operate within the tumor vasculature. In this context, the results obtained by our group on the novel role of the adhesion molecule L1 in tumor-associated vasculature [41], as described later in the introduction, provides a strong rationale for exploring this molecule as a new target.

1. 1. 5 Novel anti-angiogenic targets: the perivascular niches of cancer stem cells.

In the last years, several studies demonstrated a pivotal role of cancer stem cells (CSCs) in promoting tumor growth and metastasis [42] . CSCs consist of a rare cell population within the tumor mass and are multipotent, self-renewing and capable of generating the entire variety of cell types present in a tumor [43]. Importantly, CSCs are often quiescent and therefore may not be affected by therapies targeting rapidly dividing cells. Moreover, CSCs usually express transporters that pump out chemotherapeutic agents [44] and posses an increased capacity to repair DNA damage [45], allowing them to survive to conventional chemotherapy. These peculiar characteristics may help explaining why such therapies often fail in clinics: although they are able to destroy the tumor bulk, they cannot prevent the surviving of CSCs, thus accounting for metastasis and relapse [46].

Another peculiar characteristic of CSCs is that they are usually found in a specialized microenvironment called "niches" which provide CSCs with survival and proliferation-promoting factors. In some tumor types, such as head and neck squamous cell carcinomas [47] and brain tumors [48], CSCs reside in perivascular niches where the existence of a cross-talk between CSCs and endothelial cells is crucial for their survival [47]. Moreover, the perivascular niche can also protect CSCs from chemotherapy, thus enhancing the probability of tumor relapse.

These discoveries open novel therapeutic option for CSC-driven tumors (such as ovarian cancer, as discussed below). Moreover, the pharmacological blockade of the cross-talk between ECs and CSCs within the perivascular niche may represent a novel therapeutic opportunity for cancer patients. In this context, anti-angiogenic drugs may have a double therapeutic effect: they can target both ECs and their cross-talk with CSCs, thus preventing not only the formation of new tumor-associated vessels but also ablating the fraction of

self-renewing cells within the tumors, resulting in the repression of tumor growth [49] (Figure. 8).

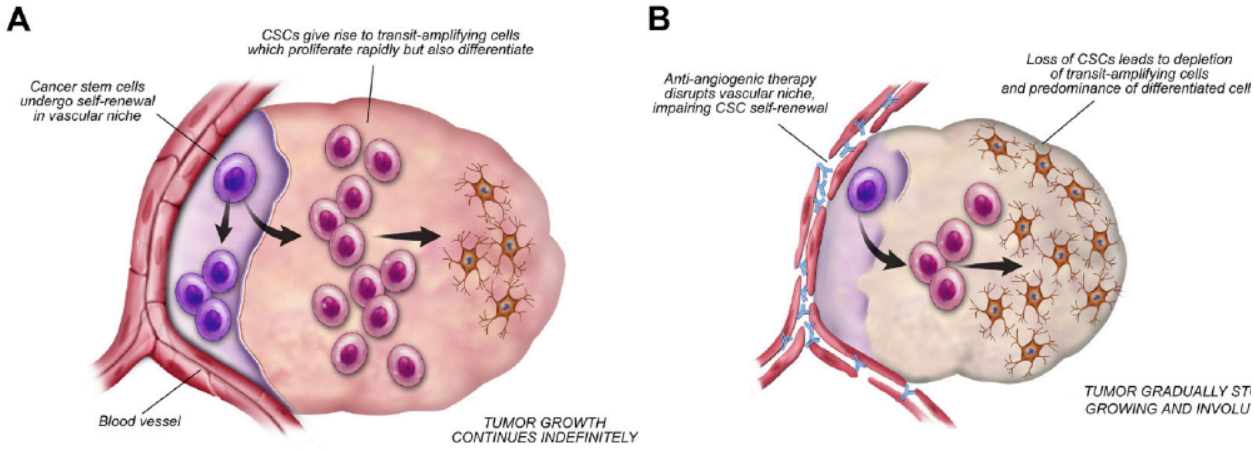

Figure 8. ***The perivascular niche of cancer stem cells: a novel target for anti-angiogenic therapy.***

CSCs reside in niches in close proximity with blood vessels and continuously receive survival signal from these specialized microenvironment (A) CSCs undergo self-renewal to maintain the CSCs pool but are also able to generate transit-amplifying cells that proliferate while acquiring a differentiated phenotype. The unceasing onset of differentiated tumor cells foster tumor growth. (B) The anti-angiogenic therapy targeting blood vessels might disrupt the CSCs niche, blocking the cross-talk between blood vessels and CSCs. The CSC pool might be exhausted (Adapted from Zeng-Jie Yang & Robert J. Wechsler-Reya 2011, [49]).

1. 2 Ovarian cancer: cancer types and cell of origin

Ovarian cancer (OC) is the second most common and the most lethal gynecological malignancy in developed countries. No specific symptoms are associated to the early phase of the disease and, therefore, the majority of OC is already at advanced stage at the time of diagnosis, with massive peritoneal spread of tumor as well as ascitic fluid [50].

Based on a series of morphologic and molecular genetic studies, Shih and Kurman proposed a dualistic model to classify ovarian carcinomas into type I and type II tumors [51].

Type I tumors include low-grade serous carcinoma, low-grade endometrioid, clear cell and mucinous carcinoma. These tumors are usually diagnosed at early stage, in most cases they grow slowly and are not clinically aggressive. At the molecular level, type I tumors are characterized by mutation in *KRAS, BRAF, PTEN, PIK3CA* and *BCL2*. Type II OCs, instead, are mostly represented by high-grade serous carcinoma but include also high-grade endometrioid carcinomas, carcinosarcomas and undifferentiated carcinomas. They are highly aggressive and usually exhibit *TP53* mutation and high genomic instability [52,53]. The ovarian surface epithelium (OSE), which is a layer of simple squamous-to-cuboidal epithelial cells covering the ovary, has long been thought to be the unique source of OC (Figure. 9A and 9B).

In 1971 Fathalla formulated the "incessant ovulation hypothesis" [54] where he stated a possible relationship between the repeated involvements of the ovarian surface epithelium in the process of ovulation and the development of the epithelial OC [54]. Indeed, every ovulation induces a wound in the OSE that must be repaired by postovulation mitosis and cell proliferation mechanisms, thus increasing the probability of alterations in the DNA repair mechanisms and the selection of putative carcinogenic mutations [55]. Over the time, this model has expanded and mediators of inflammation and hormones have been described as carcinogenesis-promoting factors. Indeed, with the release of an oocyte with its adherent cumulus granulosa cells into the adjacent fallopian tube, both the ovarian surface and the tubal fimbria are bathed with follicular fluid abundant of inflammatory cytokines, reactive oxygen species, and steroids [56,57]. Furthermore, due to the cyclic ovulation-induced rupture, the OSE was supposed to invaginate into the underlying stroma thus forming inclusion cysts. Subsequently, metaplastic changes would promote the acquisition of a "müllerian phenotype" by epithelial cells [58], thus leading to the development of the different cell types, which morphologically resemble the epithelia of the fallopian tube in high-grade serous OC, the endometrial epithelium in endometrioid OC, and the gastrointestinal tract or endocervix epithelium in mucinous OC (Figure. 9B).

However, the normal ovary does not have any cellular components would act as precursors of those tumor cell types. In fact, while cervix, endometrium and fallopian tubes derive from the müllerian ducts, the ovaries develop from mesodermal epithelium of the urogenital ridge [52,59]. Therefore, a more recent theory proposes the distal portion of the fallopian tube, that is the fimbriae epithelium, as an alternative source of OC cells (Figure. 9A and 9C). The first evidence in favor of such a theory came from the pathological examination of the fallopian tubes derived from prophylactic salpingo-oophorectomies carried out in high-risk OC patients. A meticulous sectioning of the entire tube led the to the discovery of foci of in situ tubal intraepithelial carcinoma (TIC) [53,60,61]. It was then hypothesized that malignant cells shed from the occult tubal carcinoma onto the ovaries where they can implant and form a tumor mass, which resembles a primary ovarian carcinoma. Moreover, tumor cells can also directly colonize the abdominal cavity from the tube, thus explaining the recurring peritoneal dissemination of high-grade OC and the presence of ascitic fluid in patients at the time of diagnosis.

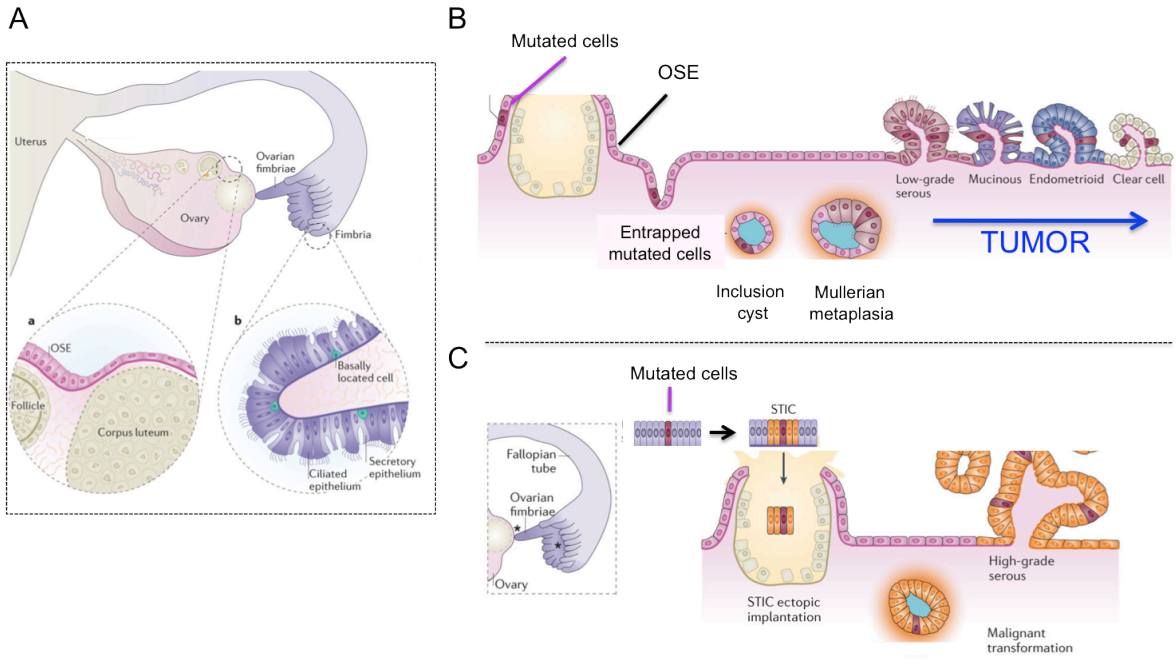

Figure 9. ***Possible origins of ovarian cancer cells.***

A) Organization and anatomy of the adult human ovary and the fallopian tube. The ovary and the fimbriae are anatomically contiguous. The ovary is lined by a monolayer of

ovarian surface epithelium (OSE). The adult fimbrial epithelium comprises two epithelial cell types: ciliated cells and secretory cells. B) Derivation of OC from OSE. OSE invaginates and forms an inclusion cyst. Due to metaplastic changes, ephithelial cells might become neoplastic and form a tumor mass in the ovary. C) Derivation of OC from fimbriae ephithelium. An in situ intra-ephithelial carcinoma (STIC) might develop in the fimbriae and, thereafter, transformed cells can be released onto the ovary and generate a tumor mass (Adapted from Annie Ng and Nick Barker 2015 [62]).

1. 2. 1 Epithelial-mesenchymal transition and stem cells in ovarian cancer

Debulking surgery followed by platinum/taxane therapy is the standard treatment for advanced ovarian cancer patients. Despite most patients show a good response to the chemotherapy, 60% to 80% of women with advanced OC eventually relapse and develop drug-resistant disease. OC patients typically survive only for 16-21 months, succumbing to metastatic spread of the disease.

Although the mechanisms of OC chemoresistance are still poorly understood, several studies have implicated the epithelial-mesenchymal (EMT) transition and cancer stem cells (CSCs) in the development of resistance to therapy and the consequent tumor relapse and metastasis [63]. Moreover, the two biological phenomena appear to be intimately connected, as EMT not only is a frequent hallmark of CSCs, but it has been shown to be causally involved in the acquisition of CSC traits [42,64].

EMT is a biological reversible process by which epithelial cells acquire mesenchymal properties, such as migratory activity. During embryogenesis, epithelial cells acquire mesenchymal markers to migrate through the extracellular environment and colonize other organs, giving rise to endoderm, esoderm and mobile neural crest cells. In cancer, instead, EMT is associated with the acquisition of an invasive phenotype by cancer cells and their ability to disseminate from the primary mass, by regulating the production of matrix metalloproteases and altering the cytoskeletal organization [63]. At the molecular level, EMT occurs through the up-regulation of several EMT-inducing transcriptional factors (EMT-

TFs) such as Snail1, Snail2, Zeb1, Zeb2, Twist, Klf8, and the modulation of adhesion molecules and cytoskeletal components, including N-cadherin, E-cadherin, Cytokeratins, Claudins and Occludin [42,65].

Several studies have demonstrated a pivotal role of EMT in acquired invasiveness and metastatic potential of OC cells. Takai and colleagues analyzed 174 primary tumors and 34 metastases of OC by immunohistochemistry. They showed that the reduction in E-cadherin expression together with the up-regulation of Snail correlated with more peritoneal metastasis and decreased PFS and OS in OC patients [66]. Moreover, several studies in OC cell lines demonstrated that the exposure of OC cells to chemotherapeutic agents induced EMT and chemoresistance [67,68]. The correlation between acquired chemoresistance and the expression of EMT markers have also been confirmed in primary OC samples. Indeed, Davidson et al identified a panel of EMT- and CSC-related genes as markers of poor chemoresponse in metastatic serous OC effusion [69].

In addition to EMT process, accumulating evidence indicates that the existence of a small population of CSCs within the tumor mass is intimately correlated with OC progression, chemoresistance and tumor relapse [42]. A variety of strategies have been tested to identify and isolate OCSCs from OC cell lines and primary samples [70-73]. A number of cell surface markers have been proposed to isolate subpopulations of cells enriched for OCSCs.

CD133 glycoprotein has emerged as one of the most promising CSC marker in EOC. CD133+ cells showed an increased tumorigenic potential as compared with CD133- counterpart in immunocompromised mice and they possessed an increased resistance to platinum-based therapy *in vitro* [70]. In addition, CD133 expression correlated also with decreased response to chemotherapy [74]. However, the results obtained using CD133 as a putative marker of CSCs are conflicting. Indeed, Kusumbe and coworkers demonstrated that CD133-expressing ovarian cancer cells are not tumorigenic *per se* but they augmented tumor development and progression by contributing to the development of tumor vasculature [75].

Other groups have proposed aldehyde dehydrogenases (ALDHs), a family of NADP-dependent enzymes that catalyze the oxidation of a broad spectrum of aldehydes, as promising markers for the isolation of OCSCs. Landen et al isolated for the first time ALDH+ OCSC and showed that high level of ALDH activity correlated with poor outcome in OC patients [72]. Moreover, in 2011 Silva et al demonstrated that few ALDH/CD133 double positive OCSC isolated from human tumor possessed tumor initiation capability in mice and that their presence in primary OC samples correlated with reduced disease-free survival (DFS) and OS [76].

In spite of the significant efforts devoted to the identification of strategy and markers to identify, isolate and target OCSCs, the results obtained so far are mostly inconsistent and unequivocal markers of OCSC are still missing. A deeper understanding of the biology of EMT and CSC in the development of OC and in its response to therapy may direct tumor research towards novel EMT/CSC targets, hopefully leading to innovative targeted therapy.

1. 2. 2 Anti-angiogenic drugs in ovarian cancer

The current standard of frontline therapy for OC patients is represented by combination surgery and cytotoxic chemotherapy. However, the approval of Bevacizumab in 2004 for the treatments of cancer patients had represented a novel therapeutic opportunity also for OC patients. In gynecological cancer, four phase-III clinical trials have been performed: the Gynecologic Oncology Group 218 (GOG-218) and the Gynecologic Cancer InterGroup International Collaboration on Ovarian Neoplasms 7 (GCIG ICON7) in first-line setting, and the OCEANS and AURELIA in recurrent setting [77].

The GOG-218 trial enrolled 1873 women with previously untreated stage III or stage IV epithelial ovarian cancer, primary peritoneal or fallopian tube carcinoma. It was a three arms trial where patients received carboplatin and paclitaxel (CT) together with concomitant and maintenance placebo (control group), or concomitant Bevacizumab and

maintenance placebo (the Bevacizumab-initiation group), or concomitant and maintenance Bevacizumab (the initiation-throughout group). This study showed an increase in the progression free survival (PSF) from 10.6 months in control group to 11.2 months in the Bevacizumab-initiation group and to 14.1 months in the initiation-throughout group [77].

The two-arm trial GCIG ICON7 enrolled 1528 women with high-risk early-stage and advanced epithelial OC, primary peritoneal or fallopian tube carcinoma. Patients were treated with CT with/without concurrent and maintenance Bevacizumab. Also in this study the addition of Bevacizumab to the standard therapy increased the PFS of OC patients from 20.3 to 21.8 months.

In recurrent setting, instead, the OCEANS trial enrolled 484 patients with platinum-sensitive OC. Patients were randomized to gentamicine and carboplatinum plus either placebo or Bevacizumab. The addition of the anti-angiogenic drug to chemotherapy increased the median PFS from 8.4 to 12.4 months. In the AURELIA trail, 361 women with platinum-resistant OC were randomized to six arms: paclitaxel, topotecan, liposomal doxorubicin with or without Becacizumab. The addition of Bevacizumab to chemotherapy double the median PFS.

Another anti-angiogenic therapeutic opportunity for OC patient could be represented by the VEGF receptor tyrosine kinase inhibitors, such as Cediranib [78] and Pazopanib [79]. These small molecule inhibitors gave some same clinical benefits in terms of improved PFS even if with noted side effects. However, in none of these trials the addition of the anti-angiogenic drug to CT did induce an increase in OS since the vast majority of OC patients became unresponsive to anti-angiogenic therapy shortly after the initiation of the therapy.

In addition to reduced neovascularization and tumor burden, in preclinical models anti-VEGF drugs seem to reduce the amount of ascitic fluid in the abdominal cavity, a well known hallmark of late-stage OC [80]. The massive accumulation of peritoneal ascites is due to the obstruction of lymphatic vessels by tumor masses and the increased leakiness of

tumor microvasculature [81]. The ascitic fluid also acts as a reservoir for growth factors, cytokines and chemokines, that foster OC growth by inducing cancer cell proliferation and tumor angiogenesis, and by preventing immunosurveillance [82]. The current treatment of malignant ascites is represented by standard chemotherapy. Once the tumor becomes resistant to therapy and relapses, the majority of patients undergo paracentesis procedure to alleviate ascites-related symptoms such as abdominal pain. VEGF-based anti-angiogenic drug gave encouraging results also in clinical setting. Indeed, the use of Bevacizumab promoted symptomatic relief of ascites [83,84]. However, in all patients ascites reformed after few months. Moreover, no randomized trials using Bevacizumab specifically for the elimination of ascites have yet been reported.

Another encouraging result came from a phase-II clinical trials using the VEGF-trap aflibercept, a drug that is able to bind VEGF and placental growth factor (PlGF). It significantly prolonged the median time to paracentesis [85], yet with high morbidity. Even though the contribution of current angiogenic-drug for the eradication of ascites is unclear and unsatisfactory [86,87] , tumor angiogenesis and the high permeability of tumor vasculature seem intimately linked to the ascites formation. Thus, the anti-angiogenic therapy might represent a promising strategy to manage ascites formation and its related symptoms in OC patients.

Overall, in order to improve the clinical benefits derived from the addition of anti-angiogenic drug to chemotherapy for the treatment of OC, it has to be taken into account that OC is a highly heterogeneous disease. Indeed, epithelial ovarian cancers are classified into five main immunohistological subtypes that differ in term of chemosensitivity, overall survival and driver genetic mutations. Despite these differences, the vast majority of clinical trials have been performed in unselected cohort of patients. Future strategies to design the suitable patient population to be treated with a defined drug, together with the identification of additional molecular pathways, could offer novel therapeutic opportunities

to overcome these limitations, especially for a tumor with high mortality rate such as OC [88].

1. 3 The cell adhesion molecule L1: a novel player in tumor-associated vasculature

L1-cell adhesion molecule (L1CAM or L1) is a 200-220 KDa transmembrane protein that belongs to the immunoglobulin superfamily [89]. It is composed by an extracellular portion, which contains six Ig-like domains and five fibronectin type III repeats (FNIII-like), a transmembrane region and a short cytoplasmic tail [89] (Figure. 10). L1 is involved in homophilic and heterophilic interactions on the cell surface. Partners of L1 heterophilic interactions include integrins and receptor tyrosine kinases (RTKs), such as fibroblast growth factor receptor (FGFR). These interactions have functional implications, for example modulating cell motility and signal transduction [90].

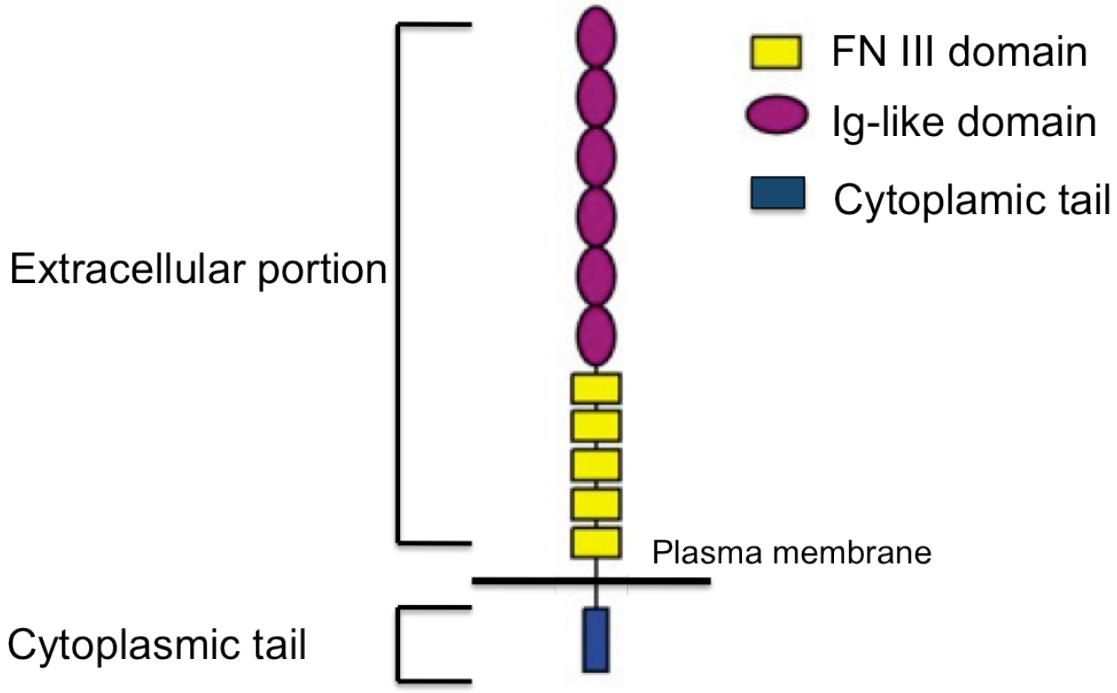

Figure 10. ***L1 structure***

L1 cell adhesion molecule belongs to immunoglobulin super-family. It is composed by six Ig-like domains (purple), five fibronectin type-III repeats (FNIII domain, yellow), a transmembrane region and a conserved cytoplasmic tail (blue) (Adapted from Chun Hua Wei & Seong Eon Ryu 2012, [91]).

L1 can undergo membrane-proximal cleavage by a disintegrin and metalloproteinases (ADAMs), which generates a soluble 200-kDa ectodomain and a membrane-retained stub of 32 kDa [92]. The shedding of the ectodomain occurs at the surface of normal and tumor cells but also in cell-derived vesicles, called exosomes [93]. Moreover the soluble ectodomain of L1 is biologically active: it promotes cell migration [94], protects cell from apoptosis [95] and stimulates angiogenesis [96]. The membrane-retained cytoplasmic tail is a substrate of γ-secretase, which, upon cleavage of the intra-membrane portion, releases a soluble L1 intracellular domain that is able to translocate into the nucleus and regulate gene transcription [97] (Figure. 11).

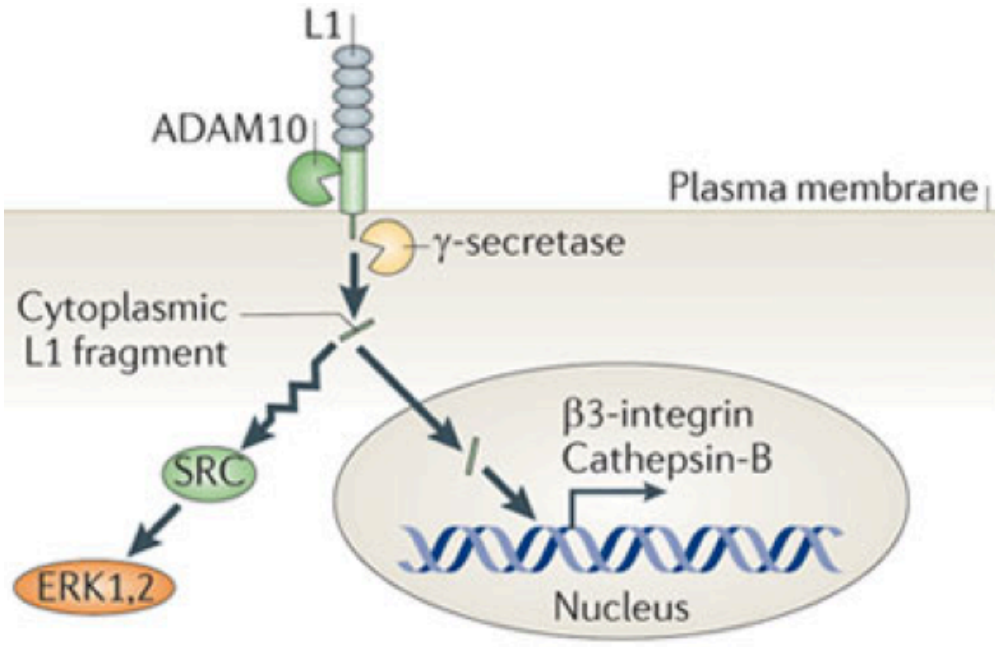

Figure 11. ***L1 processing at the plasma membrane.***

At plasma membrane L1 undergoes to proteolytic cleavage of the extracellular domain that results in the shedding of the extracellular portion of the protein. The membrane-retained intracellular tail is further processed by g-secretase. This second cleavage results in the formation of a soluble cytoplasmic tail that is able to translocate from the cytoplasm to the nucleus where it regulates gene transcription (Adapted from Cavallaro U & Dejana E. 2011, [98]).

L1 was initially characterized as an adhesion molecule playing a key role in the development of nervous system [99]. Thereafter, several studies reported the expression of L1 in different cell types, such as immune cells [100] and tumor cells [101]. Indeed, it was demonstrated that the aberrant expression of L1 in various cancer types, including endometrial carcinoma, pancreatic ductal carcinoma, melanoma and glioblastoma, correlates with tumor malignancy and poor prognosis [97].

In OC, the expression of L1 is frequently increased in high-grade serous tumor while it is absent in the normal counterpart [93], and its expression correlates with the risk for suboptimal debulking [102]. In OC patients, soluble L1 can also be detected in serum and

ascitic fluid [93], and the expression of L1 in tumor cells correlates with higher level of soluble L1 released in the ascitic fluid, which might imply a functional role of the ectodomain fragment in OC. Of note, L1 shedding represents an unfavorable indicator for OC response to chemotherapy and patient survival [93,102].

Several studies demonstrated a role of L1 in various cellular processes related to tumorigenesis such as invasiveness and migration [97], thus supporting the metastatic spread, as well as chemoresistance. Accordingly, inhibition of L1 by RNA interference or antibody-mediated blockade reduced migration and proliferation of ovarian tumor cells *in vitro* [95,103,104]. Furthermore, treatment of OC mouse models with L1-neutralizing antibodies reduced tumor burden and decreased ascites volume [105,106]. Finally, the combined treatment of OC-bearing mice with L1 antibody and paclitaxel improved the therapeutic response [107].

Within a tumor, the neoplastic cells are by no means the only cell type where L1 can be found. Indeed, our group has analyzed a wide range of solid tumors and showed that L1 is commonly expressed in the cancer-associated vasculature, while it is almost absent in normal vessels [100]. Besides confirming previous scattered reports on the expression of L1 in tumor vasculature of breast, ovarian, colon and pancreatic carcinoma [100,108], these results point to L1 as a potential marker of pathological angiogenesis. Furthermore, by combining genetically manipulated mouse tumor models with *in vitro* endothelial cell biology studies, we have recently discovered a novel, pleiotropic role of L1 in tumor vasculature, which implicates this molecule in cancer neovascularization and in the dysregulation of cancer vessel integrity and function (See background and rationale) [41].

Overall, the cell surface localization of L1 together with its specific upregulation in tumor-associated vasculature, make it a possible marker of advanced stage cancer as well as a potential candidate for novel anti-angiogenic therapy to fight incurable and aggressive human tumors, such as OC.

2. MATERIALS & METHODS

2. 1 Cell lines

Mouse lung-derived ECs (luECs), were immortalized with polyoma middle T antigen as previously described [109] and cultured in MCDB131 medium (Gibco) supplemented with 20% North American (NA) Fetal Bovine Serum (FBS) (Invitrogen), 2 mM L-Glutamine (Lonza), 1 mM Na-pyruvate (Gibco), 100 μg/ml heparin (Sigma), 50 μg/ml EC growth supplement (ECGS) obtained from calf brain. ECs were seeded on 0.1% gelatin (Sigma) and cultured at 37°C in humidified atmosphere with 5% CO_2. Where indicated, EC adhesion was enhanced by coating tissue culture plates with glutaraldehyde–crosslinked gelatin, as follows. Plates were incubated overnight with 1% gelatin at 37°C followed by a crosslinking with 2% glutaraldehyde for 15 minutes at room temperature (RT). Glutaraldehyde was replaced with 70% ethanol for 1 hour at RT. After 5 washes with PBS (Lonza), plates were incubated for 2 hours at 37°C with 2 mM glycine in PBS (Lonza). Prior to cell seeding, plates were washed 5 times with PBS (Lonza).

luECs expressing full length murine L1 (luEC-L1) and the control cells (luEC-mock) were obtained as previously described [41].

ID8 cells, a spontaneously transformed mouse ovarian cancer cell line, were cultured in DMEM (Lonza), 5% FBS (Invitrogen), 2mM L-Glutamine (Lonza).

B16-F10 melanoma cell line, was cultured in DMEM (Lonza), 10% FBS (Invitrogen), 2mM L-Glutamine (Lonza).

HEK293 cells were cultured in DMEM (Lonza), 10% FBS (Invitrogen), 2mM L-Glutamine (Lonza).

2. 2 Mice

$L1^{floxed}$ and Tie2-Cre mice were generated in the C57BL/6 genetic background as

previously described [100]. To obtain Tie2-Cre; $L1^{fl/\ fl}$ females, $L1^{fl/fl}$ females were crossed with Tie2-Cre;$L1^{fl}$ male mice. Genomic DNA of the offspring was isolated from tail biopsies and the genotype was determined by PCR analysis for Tie2 gene (see below).

NOD/SCID/IL2Rg^{null} female mice were purchased from Charles River Laboratories.

2. 3 Mouse genotyping

Tail tips were washed in Ethanol 100% and in PBS (Lonza) and then digested in Digestion Buffer (16.6 mM Ammonium Sulfate, 0.5 mM ß- 2-mercaptoethanol, 0.05 M EDTA pH8, 0.15 M Tris-HCl pH 8.8, 570 ug/mL Proteinase-K (Sigma), 10% Triton-X100 in water) shaking, overnight at 55 °C. Proteinase-K was inactivated by high temperature (95°C, 20 minutes).

Digested tails were centrifuged at 12,000 g for 5 minutes at RT and 2 μL of supernatant was used for the PCR analysis for the Tie2 promoter.

Primer forward: CCAAAATTTGCCTGCATTACCGGTCGATGC;

Primer reverse: ATCCAGGTTACGGATATAGT.

2. 4 *In vivo* models

2. 4. 1 Syngeneic mouse model of ovarian cancer

The syngeneic mouse model of ovarian cancer has been described previously [110]. Briefly, one million of ID8 ovarian carcinoma cells stably expressing GFP were injected intra-peritoneally into 8-10 week old female mice. One month after the injection, animals were sacrificed and tumor dissemination into the abdominal cavity was measured by fluorescent stereomicroscope. In particular, the abdominal wall, omentum and diaphragm were analyzed by stereomicroscopy for GFP-positive implants. For each organs, picture of GFP-positive implants were taken. The number of tumor implants was counted as described in paragraph 2. 5). Then, all the organs were embedded in Killik cryostat embedding medium

(Bio-Optica 05-9801) and stored at -80 °C for *ex-vivo* analysis.

2. 4. 2 CO-transplantation of ID8 cells and luECs

GFP-expressing ID8 cells were mixed with luEC-L1 or luEC-mock (two ratios tested, $1x10^6$:$1x10^6$ or $5x10^5$:$1x1^5$) and were transplanted subcutaneously in 8-10 week old NOD/SCID/IL2Rg^{null} female mice in a final volume of 160 uL (1:1 with Matrigel, Cat. 356231, Corning). When tumors reached the size of 450 mm^3, animals were sacrificed and tumors were digested in Digestion Buffer (HAM's F12+DMEM 2mM L-Glutamine, 200U/mL Collagenase IA and 100 U/mL Hyaluronidase) for 2 hours at 37°C in order to obtain a single cell suspension. GFP-expressing ID8 cells were then isolated from digested tumors by FACS sorting (BD Influx Cell Sorter 646500). $2x10^4$ cells were re-transplanted subcutaneously into 8-10 week old NOD/SCID/IL2Rg^{null} female mice. Tumor growth was assessed two times per week by caliper measurements. Tumor volumes were recorded at the indicated time points and calculated using the formula V = (d*d*D/2), where d and D are the minor and the major tumor axis, respectively.

2. 4. 3 CO-transplantation of ID8 cells and conditioned medium (CM) derived from endothelial cells

Conditioned medium derived from luEC-L1 (luEC-L1-derived CM) and from luEC-mock (luEC-mock-derived CM) was prepared in MCDB 131 medium (Gibco) without serum, it was collected after 48-60 hours of culture and was centrifuged at maximal speed for 10 minutes. 10^6 GFP-expressing ID8 cells were transplanted subcutaneously in NOD/SCID/IL2Rg^{null} female mice (8-10 week old female mice) together with 50 μl of luEC-L1-derived CM or luEC-mock-derived CM and 50 μl Matrigel Matrix (Cat. 356231, Corning). Tumor growth was assessed one time per week by caliper measurements. Tumors volumes were recorded at the indicated time points and calculated as reported

above.

2. 5 Quantitation of tumor implants

In order to quantify GFP-expressing ID8-derived tumor implants in an unbiased way, we adopted the "*Otsu Method"* (IEEE TRANSACTIONS ON SYSTEMS, MAN, AND CYBERNETICS, VOL. SMC-9, No.1, JANI'ARY 1979), which is an algorithm used to automatically perform image thresholding. Any image is composed by pixels with different intensity values, ranging from 0 to 255 (for 8-bit images). This method allows stratifying all pixels into two levels: a foreground (GFP-signal) and a background.

The *Otsu method* calculates the optimal threshold able to separate the foreground and the background so that their intra-class variance is maximal. For each organ, the best threshold was determined and then the number of GFP-expressing tumor implants was counted using a custom-made macro of ImageJ software. This macro identifies the GFP-positive lesions in each organ and counts them. The final output of this analysis is the number of tumor implants per organ.

2. 6 Cell migration assay

To assess cell migration, we employed the wound-healing assay. luECs were seeded on fibronectin-coated (1 **μ**g/cm2) 24-well plates. Confluent monolayers of luECs were starved for 24 hours in MCDB131 medium (Gibco) containing 0.5% FBS. Monolayers were wounded with a plastic pipette tip to induce EC migration into the wound. Where indicated, cells were treated for 2 hours with 100 nM FGFR inhibitor PD173074 or vehicle only (DMSO). Images of the wounds were acquired at 0 and 24 hours. The width of the wounds was measured with ImageJ software, and the distance covered by luECs, expressed as μm in 24 hours, was calculated according to this formula: (wound width at 0 – wound width at 24 hours).

2. 7 Cell proliferation assay

ECs were seeded at a density of $2x10^3$ cells/well in 96-well plates coated with glutaraldehyde–crosslinked gelatin. After overnight incubation in medium containing 5% FBS, cells were stimulated with medium containing 20% FBS, 100 μg/ml heparin, and 50 μg/ml ECGS. Where indicated, cells were treated with 100 nM FGFR inhibitor PD173074 or vehicle only (DMSO). Cells were fixed at 0, 24, 48, and 72 hours, followed by staining with 0.1% crystal violet in 20% methanol. Bound dye was solubilized with 10% acetic acid, and the absorbance at 590 nm was measured. Cell growth was normalized on absorbance measured at 0 hours.

2. 8 Tube formation assay

Matrigel-based tubulogenesis assay was performed to assess the ability of ECs to form capillary-like structures. Confluent ECs were starved overnight with medium containing 1% FBS. Growth factor-reduced Matrigel was thawed overnight at 4°C on ice and, the day of the assay, 50 uL of Matrigel were plated on the bottom of 96-well plate and left at 37°C for 1 hour for gelification. Thereafter, $1x10^4$ cell/well were seeded on Matrigel and incubated at 37 °C. Optical images of the wells were acquired after 7 hours at 4X magnification using EVOS FL Imaging System. The tubes in each well were manually counted. The experiments were performed in triplicates and repeated three times.

2. 9 Antibodies

The following antibodies were used as indicated:

Mouse anti-human L1 (clone UJ127; 1:30 in IHC on human tissues; Thermo Scientific);

Purified anti–mouse CD31 (clone MEC 13.3; 1:50 in IF on mouse tissues, Santa Cruz);

Rabbit anti-mouse L1 728 (polyclonal antibody against mouse L1-Fc produced in our lab, [41]);

Rat anti IL-6 antibody (Clone MP5-20F3; Cat. 504506, BioLegend);

IgG from rat serum (I4131, Sigma).

Secondary antibodies for immunofluorescence analyses: Cy3-conjugated donkey anti-rabbit (Li-Starfish, 1:500); Cy5-conjugated donkey anti-rat (Li-Starfish, 1:500).

Secondary antibodies for immunoblot analysis: HRP-linked goat anti-rabbit (1:3000, BioRad).

2. 10 Immunoprecipitation

LuEC-L1- and luEC-mock-derived CM was prepared as described in paragraph 2. 4. 3.

2 mL of CM was added with 30 μL of rec-Protein G-sepharose 4B Conjugate (10-1242, Invitrogen) and 5 μg of rat IgG for medium pre-clearing and leaved 1 hour at 4°C under rotation. At the end of the incubation, medium was centrifuged at maximal speed for 1 minute and it was divided in two parts. 1 mL of medium was incubated with 3.3 μg of rat anti IL-6 antibody for 2 hours at 4°C under rotation and 1 mL with 3.3 μg of rat IgG, as control.

Therefore, 20 μL of rec-Protein G-sepharose 4B Conjugate (10-1242, Invitrogen) was added and samples were left 2 hours at 4°C under rotation.

The IL6-depleted medium was used for the sphere assay (See section 2.18).

2. 11 Immunoblotting

Proteins were extracted from ID8 and B16-F10 cells using RIPA lysis buffer (0.1% SDS, 0.5% DOC, 1% TritonX-100, 150mM NaCl, 50 mM Tris pH 7.4). Cell extracts were sonicated and then centrifuged for 5 minutes at 12,000 g to discard cell debris. The supernatants were collected, and the concentration of protein was determined using Bio-Rad Protein Assay Dye Reagent Concentrate (Cat. 500-0006, Bio-Rad) according to the manufacturer's instructions. 25 ug of protein were separated on SDS polyacrylamide gel

(SDS-PAGE) and blotted on nitrocellulose membranes using Trans-Blot Turbo Transfer Pack (BIO-RAD). Membranes were incubated in blocking solution (TBS, 0.1% Tween 20 containing 5% nonfat milk) for 2 hour at RT and then overnight at 4°C with primary antibodies diluted in blocking solution. Membranes were then incubated with horseradish peroxidase–conjugated secondary antibodies (BIO-RAD) and the signal was detected by the Clarity Western ECL Substrate (BIO-RAD) and acquired using Chemidoc (Universal hood II, Bio-rad).

2. 12 Immunofluorescence

ID8 tumors were embedded in Killik cryostat embedding medium (Bio-Optica 05-9801). Tumor sections (3 μm) were fixed 10 minutes in 4% paraformaldehyde (PFA) and incubated for 1 hour at RT with a blocking solution (PBS (Lonza), 2% bovine serum albumin (BSA), 5% donkey serum, and 0.05% Triton X-100). Samples were then incubated 2 hours with primary antibody diluted in blocking buffer, followed by the incubation with secondary antibody (45 minutes at RT). Samples were then washed in PBS and counterstained with DAPI solution.

2. 13 Immunohystochemistry

The immunohistochemical analysis of L1 expression was carried out on different normal samples and high-grade serous ovarian carcinoma. Samples were 4% PFA-fixed and paraffin embedded. After an over-night at 37 °C, tumor sections (3 **μ**m) were deparaffinized using Leica ST5020 Multistainer according to the following protocol: bioclear (Bio-Optica Ref. 06-1782D) 15 minutes for two times, Absolute Ethanol 5 minutes for two times, 95% Ethanol 5 minutes, 70% Ethanol 5 minutes, 2 washes of 2 minutes in distilled water. According to the primary antibody used, tissue sections were treated with the antigen unmasking solution EDTA pH 8 in pre-wormed water bath a 95 °C for 50 minutes. After two washes in water, endogenous peroxidases were blocked using

3% Hydrogen peroxide solution (Carlo Erba, 412072). Tissue sections were incubated with the blocking solution (TBS, 2% BSA, 2% normal goat serum (ECS0200D/L, EuroClone), and 0.05% Triton X-100) for 1 hour. Samples were then incubated 2 hours with primary antibodies diluted in blocking buffer, followed by secondary antibodies (Dako EnVision+ System-HRP Labelled Polymer) for 30 minutes at RT. Dako chromogen substrate (Liquid DAB+ Substrate Chromogen System Ref. K3468) was used for signal detection. Samples were then washed and counterstained using Hematoxylin solution (Leica). Pictures of stained sections were acquired with the scanner Aperio ScanScope XT, 20x objective.

2. 14 H&E staining

Hemangioma sections were 4% PFA-fixed and paraffin embedded. After an overnight at 37 °C, tumor sections (3 μm) were deparaffinized using Leica ST5020 Multistainer according to the following protocol: bio-clear (Bio-Optica Ref. 06-1782D) 5 minutes for two times, absolute ethanol for 2 minutes for two times, 95% ethanol for 2 minutes, 70% ethanol 2 minutes. After two washes of 2 minutes in distilled water, tissue sections were then treated with hemalast reagent (Leica) for 30 seconds and with Hematoxylin (Leica) for 5 minutes. After one wash in water, sections were treated with differentiator solution (Leica) for 45 seconds. After one wash in water, sections were treated with bluing agent (Leica), treated with ethanol 80% for 1 minute and finally stained with eosin (Leica) for 1 minute. Hemalast, Hematoxylin, differentiator, eosin and bluing reagents were from Leica ST Infinity H&E Staining System (Leica, 3801698).

2. 15 Gene Expression profiling

ECs were seeded on plates coated with glutaraldehyde–crosslinked gelatin and cultured in complete medium for 4 days to reach confluence. Cells were treated with FGFR inhibitor PD173074 or DMSO for 2 hours and then total RNA was extracted with RNeasy Mini Kit

(QIAGEN). Quality control of the RNA samples was performed using Agilent Bioanalyzer 2100 (Agilent Technologies). Two different RNA extractions were processed for each condition. Each sample was labeled and hybridized to a Mouse Gene 1.0 ST Genechip array according to the manufacturer's instructions (Affymetrix). Data were normalized using the Robust Multi-array Average (RMA).

2. 16 RNA extraction from ID8 cells or luECs and quantitative RT-PCR analysis

ID8 cells, B16-F10 cells or luECs were cultured as described above. Total RNA was isolated by extraction with RNeasy Mini Kit (QIAGEN). 2 μg or RNA were reverse-transcribed with random hexamers (SuperScript ViloTM cDNA Synthesis Kit; Invitrogen) according to manifacturer's instructions. cDNA samples (5 ng) were amplified in triplicate with the TaqMan 710 Gene Expression Assay (Applied Biosystems) and an ABI/Prism 7900 HT thermocycler (Applied Biosystems). Preparations of RNA template without reverse transcriptase were used as negative controls.

For qRT-PCR analysis performed on ID8 and B16-F10 cell lines, gene expression level was normalized against the geometric mean of the housekeeping genes encoding for GAPDH and 18S.

For qRT-PCR analysis performed on luECs, gene expression level was normalized against the geometric mean of the housekeeping genes encoding for GAPDH and ACTB.

2. 17 RNA extraction from paraffin embedded tumors

Total RNA was extracted from 2 sections of 10 μm derived from paraffin embedded ID8-tumors following the Manufactory's protocol (AllPrep DNA/RNA FFPE, Qiagen). 2 μg or RNA were reverse-transcribed with random hexamers (SuperScript ViloTM cDNA Synthesis Kit; Invitrogen) according to manifacturer's instructions. cDNA samples (5 ng)

were amplified in triplicate with the TaqMan 710 Gene Expression Assay (Applied Biosystems) and an ABI/Prism 7900 HT thermocycler (Applied Biosystems). Preparations of RNA template without reverse transcriptase were used as negative controls.

2. 18 Sphere assay

After two washes in PBS (Lonza) to carefully eliminate serum, ID8 cells were detached from tissue-culture plate using Trypsin EDTA (BE17-161E, Lonza). Cells were counted and cultured under non-adherent condition on Poly(2-hydroxyethylmethacrylate)-treated (P3932-25G, Sigma) 6 well plates. Cells were cultured in serum-free medium (DMEM/F12, 1% PEN-STREP (Lonza), 1% L-Glutamine (Lonza), B27 supplement (Gibco), EGF 20 ng/mL, FGF 10 ng/mL) mixed with luEC-L1-derived CM or luEC-mock-derived CM in 3:1 ratio. Cells cultured in serum-free medium without CM (no CM) were used as control. For each condition 500 cells/well were plated in a final volume of 2 mL, in triplicate. After 5 days in culture, spheres were counted and the sphere forming efficiency (SFE) was calculated as the percentage of the ratio between the total number of spheres and the total number of cells seeded.

2. 19 FGFR1 silencing in luECs by shRNA

Lentiviruses were generated by transient transfection of HEK293T cells with 10 μg of four shRNA for mouse FGFR1 (GeneCopoeia, No BC033447.1) or of the scrambled control, together with the packaging vectors pMD2.G (Addgene, plasmid #12259), pRSV-Rev (Addgene, plasmid #12253), pMDLg/pRRE (Addgene, plasmid #12251), by calcium phosphate precipitation. After 24 hours of incubation at 37°C, the cell supernatants were collected 24 hours and 48 hours after transfection and filtered with a 0.45-μm filter. The lentiviral particles were added to luEC-L1 or luEC-mock (3×10^5 cells/well) cultured in gelatin-coated 6-well plates. 24 hours after infection, 2ug/mL puromycin was added to luECs in culture to select only endothelial cells efficiently transduced by shRNAs.

2. 20 Statistical analysis

Student's two-tailed t-test was used to determine the statistical significance. For *in vivo* experiments with intraperitoneal injection of ID8 cells, a Proportion Test or Poisson Rate was used to determine the statistical significance. Differences were considered significant at $p \leq 0.05$.

BACKGROUND and RATIONALE

In a paper recently published from our lab [41], we described for the first time the pivotal, cell-autonomous role of endothelial L1 in pathological vasculature. In particular, the function of L1 in tumor angiogenesis was studied in a conditional knockout mouse model. The endothelial-specific ablation of L1 in mice was achieved by crossing transgenic mice expressing Cre-recombinase under the control of the endothelial-specific Tie2 promoter [111] with $L1^{fl}$ mice carrying two floxed alleles of the *L1cam* gene [112]. The resulting Tie2-Cre;$L1^{fl}$ mice were used to set up an orthotopic, syngeneic model of pancreatic carcinoma, based on the injection of the murine pancreatic cancer cell line Panc02 into the head of the pancreas. This approach revealed that vascular L1 deficiency results in decreased tumor growth and tumor angiogenesis. Consistent with the notion that cancer-associated vasculature is irregular and disorganized (See Introduction), tumors from control mice showed impaired vascular maturation and the loss of endothelial polarity. Notably, this alterations were reverted by the mere ablation of endothelial L1, which was sufficient to promote vascular normalization, as shown by restored pericyte coverage and endothelial polarity [41], thus implicating L1 in the aberrant phenotype of cancer vessels.

These results implied that L1 could be a therapeutic target for preventing tumor neo-vascularization and the consequent dissemination of cancer cells. Indeed, the treatment of tumor-bearing mice with a polyclonal antibody against the extracellular domain of L1 led to a significant reduction of tumor growth, accompanied by decreased tumor vascularization and by vascular normalization [41].

The role of L1 in tumor vasculature was also studied *in vitro*, manipulating L1 expression in murine lung-derived endothelial cells (luECs), which express low levels of endogenous L1. In this model system, forced L1 over-expression induced cell proliferation, migration and tubulogenesis. Moreover, the gene expression profile of L1-overexpressing versus

control cells revealed a general up-regulation of genes associated with neo-vascularization and with endothelial-to-mesenchymal transition.

All these findings have provided the rationale for my PhD project, which has focused on the role of endothelial L1 as a master regulator of cancer vessel function. Since ovarian carcinoma (OC) is a tumor that is strictly dependent on angiogenesis and has shown promising results in studies with anti-angiogenic treatments, I have focused my project in studying the functional role of vascular L1 in OC and the crosstalk between the microenvironment and OC. Such a choice was also supported by the long-standing interest and expertise of our lab in this tumor type.

My PhD project aims at defining the role of vascular L1 in ovarian tumorigenesis and at dissecting L1's function in endothelial cells at the cellular and molecular level. Thus, my findings will contribute to a deeper understanding of the biological mechanisms that drive OC progression, and they may also pave the way for novel anti-angiogenic strategies that would improve the clinical management and the prognosis of OC patients.

3 RESULTS

3. 1 Endothelial L1 deficiency reduced tumor dissemination in mice

Recent work published by our group has capitalized on a mouse model of pancreatic cancer to show that endothelial L1 is causally involved in the aberrant morphology and function of tumor-associated vasculature [41]. Based on the key role that the vascular system plays in ovarian cancer (OC) development and progression [113] a crucial objective of our work is to test whether vascular L1 has a functional role in OC malignancy. To assess the clinical relevance of our approach, we first checked the expression of vascular L1 in a cohort of human OC samples. A preliminary screening on a series of samples has revealed that L1 is expressed at high level in OC vessels (Figure. 12 A and 12 C), while no or little expression was found in normal ovaries (Figure. 12 B and 12 C).

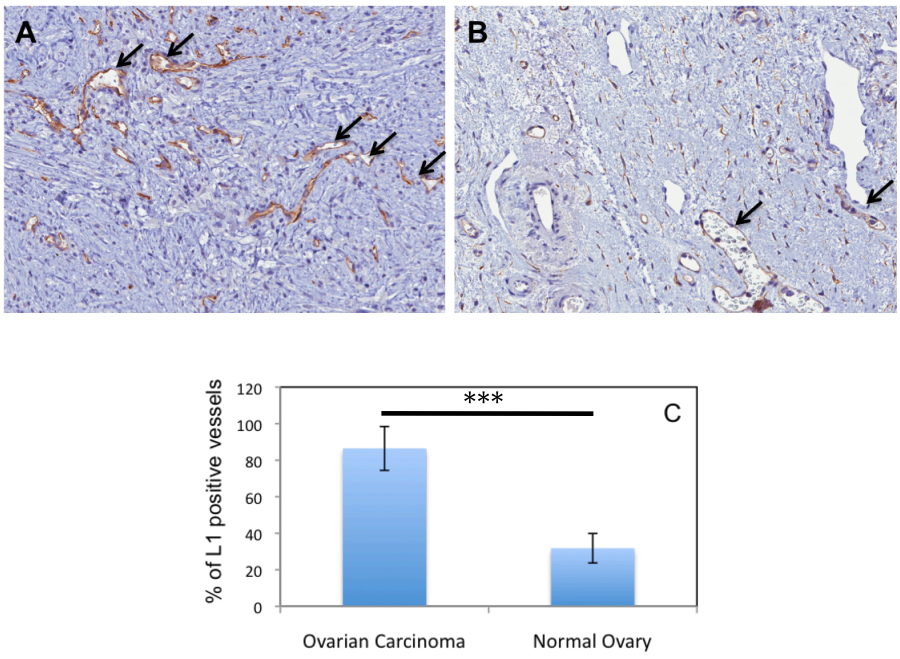

Figure 12. ***Vascular L1 expression in OC and normal ovary.***

Tissue section from human ovarian carcinoma (A) and from normal ovary (B) stained for L1. The tumor vasculature exhibits markedly higher levels of L1 (arrows) in comparison to its normal counterpart where few vessels are L1-positive. (C) Quantification of L1-expressing vessels in ovarian carcinoma and normal ovary (n=10) ***(*** p ≤ 0.005)****.*

To define the functional role of vascular L1 in OC growth and progression, the expression of L1 has been ablated in endothelial cells by crossing Tie2-Cre mice, which express Cre recombinase under the control of the Tie2 promoter [111], with mice carrying LoxP-flanked alleles of the *L1cam* gene ($L1^{fl/fl}$). The Tie2-Cre;$L1^{fl/fl}$ mouse model, extensively characterized in our lab [41,100] was combined with a syngeneic model of OC based on the murine cell line ID8, previously shown to recapitulate OC development upon orthotopic injection into recipient C57BL/6 mice [110].

Of note, ID8 cells did not express L1 endogenously, either at mRNA level (Figure. 13) or at protein level (Figure. 14). B16-F10 melanoma cell line was used as positive control for L1 expression [41]. This enabled us to focus, at least for this initial study, specifically on the role of host-derived L1 in OC growth and dissemination, ruling out the contribution (yet possible and even likely in other model systems) of tumor-derived L1.

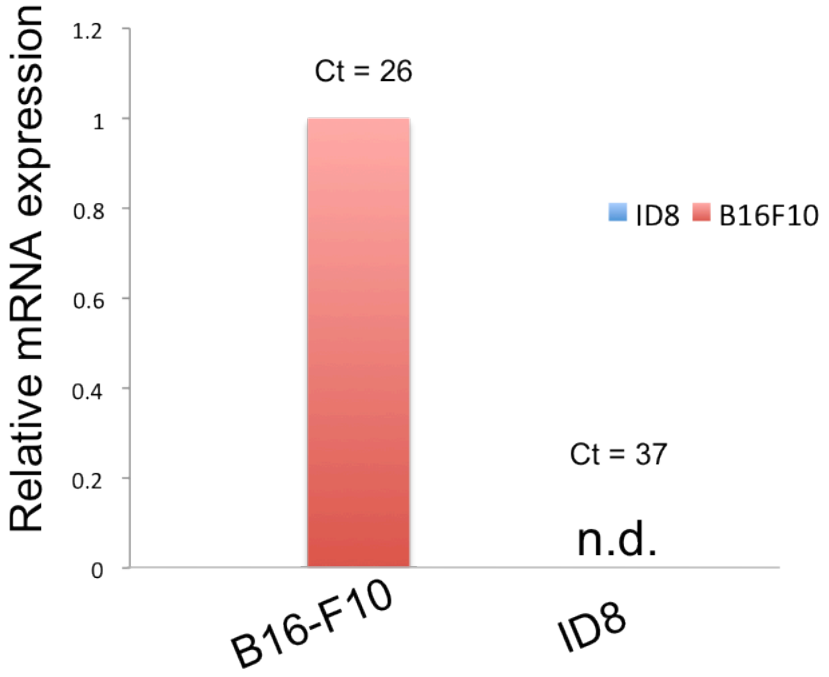

Figure 13. ***ID8 ovarian cancer cell line did not express L1 endogenously at mRNA level.***
Total RNA was extracted from ID8 cells and the expression level of L1 was measured by qRT-PCR. Results were normalized on the expression of the housekeeping genes GAPDH and 18S. Since the expression of L1 in ID8 cells was nearly undetectable (Ct=37), we used B16-F10 melanoma cells as positive control [41] *(*n.d., not detectable*).*

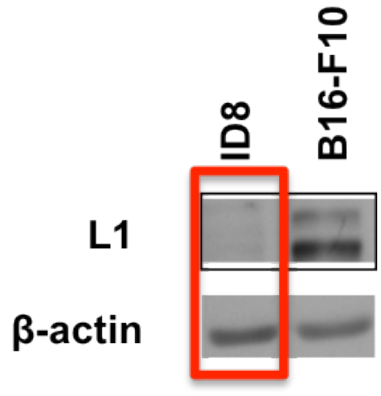

Figure 14. ***ID8 mouse ovarian cancer cell line did not express L1 protein.***
Immunoblot analysis of ID8 cells revealed that they did not express L1 protein endogenously. B16-F10 mouse melanoma cell line was used as positive control for L1 expression [41]*. b-actin served as loading control.*

The intra-peritoneal injection of ovarian cancer cells is widely used as an orthotopic model that mimic the advanced stage of the human disease, characterized by the dissemination of OC cells in the peritoneal cavity. Thus, we transplanted Tie2-Cre;L1$^{fl/fl}$ and L1$^{fl/fl}$ (control group) mice with 10^6 ID8 cells by intra-peritoneal injection. To facilitate the detection and quantitation of tumor implants in the abdominal cavity of mice, we took advantage of ID8 cells stably expressing GFP (ID8-GFP). In agreement with previous work [114], one month after the injection tumor implants were detected in several peritoneal sites, such as mesentery and abdominal wall (Figure. 15).

We first confirmed the ablation of L1 in the OC vasculature of Tie2-Cre;L1$^{fl/fl}$ by comparing Tie2-Cre;L1$^{fl/fl}$ ID8 tumor-bearing with control mice (Figure. 16). Importantly, nerves of Tie2-Cre;L1$^{fl/fl}$ mice retained the expression of L1 (Figure. 16), thus serving as an internal control and confirming the specificity of the genetic inactivation of L1 in the tumor vasculature. This phenotype was accompanied by a reduction of ID8 tumorigenicity: while 100% of control L1$^{fl/fl}$ mice developed tumors in the omentum and 87.5% in the abdominal wall, these were present only in 62.5% and 50%, respectively, of Tie2-Cre;L1$^{fl/fl}$ (Table 1). Moreover, counting GFP-expressing ID8-implants per mouse revealed a statistically significant decrease in the number of lesions in the omentum, abdominal wall and diaphragm of Tie2-Cre;L1$^{fl/fl}$ mice (Figure. 17).

All these data supported the hypothesis that vascular L1 contributes to OC malignancy and provided the rationale for exploring the underlying mechanisms.

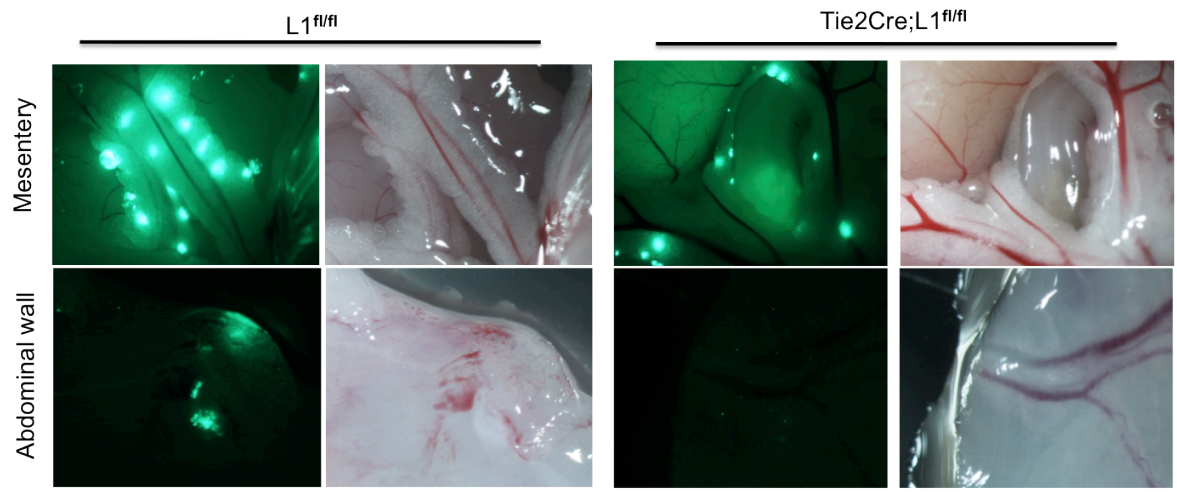

Figure 15. ***ID8-GFP based OC model.***

ID8-GFP cells were injected intra-peritoneally in $L1^{fl/fl}$ *and Tie2Cre;*$L1^{fl/fl}$ *mice. Representative images of GFP-expressing ID8 tumor implants in mesentery and abdominal wall of* $L1^{fl/fl}$ *(left panel) and Tie2Cre;*$L1^{fl/fl}$ *(right panel) mice at the time of sacrifice. ID8 model closely resemble the human disease.*

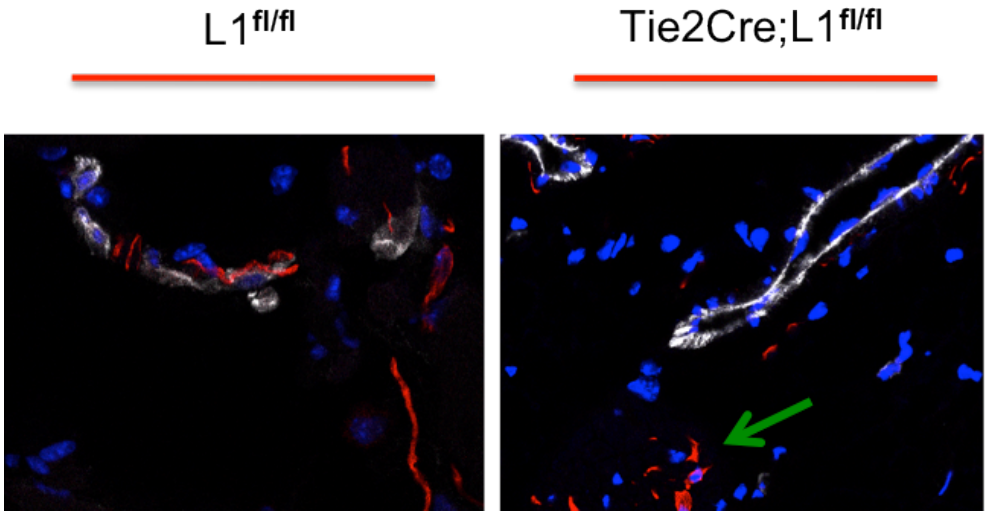

Figure 16. ***Ablation of L1 in tumor-associated vasculature of Tie2Cre;L1$^{fl/fl}$ mice***

Immunofluorescence analysis of frozen section derived from ID8 tumor implant grown on the abdominal wall of Tie2Cre;$L1^{fl/fl}$ *(right panel) and control mice (left panel). Co-staining for L1 (red) and the endothelial marker CD31 (white) showed L1-expression in tumor vessel of* $L1^{fl/fl}$ *mice while no expression was found in the vasculature of Tie2Cre;*$L1^{fl/fl}$ *tumor. The green arrow indicates L1-expressing nerves.*

Organ	$L1^{fl/fl}$	Tie2Cre; $L1^{fl/fl}$	P-value
Mesentery	8/8	8/8	/
Omentum	8/8	5/8	0.05
Abdominal wall	7/8	4/8	0.1
Diaphragm	8/8	8/8	/

Table 1. ***Vascular L1 deficiency affects tumor burden***.
$L1^{fl/fl}$ *(n=8) and Tie2Cre;* $L1^{fl/fl}$ *(n=8) mice were transplanted intraperitoneally with* 10^6 *ID8-GFP cells. Vascular L1 deficiency reduces the number of mice with tumor implants in the omentum and in the abdominal wall.*

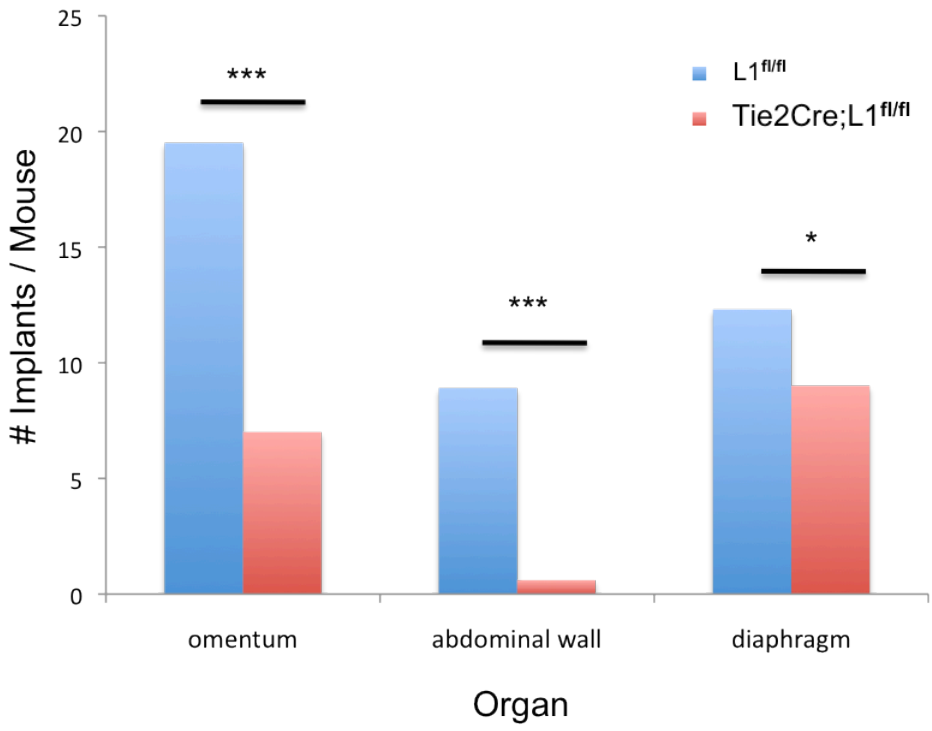

Figure 17. ***Vascular L1 deficiency affected OC peritoneal dissemination.***
$L1^{fl/fl}$ *(n=8) and Tie2Cre;*$L1^{fl/fl}$ *(n=8) mice were transplanted intra-peritoneally with* 10^6 *GFP-expressing ID8 cells. After 30 days, GFP-positive neoplastic lesions in different peritoneal organs were counted. Vascular L1 deficiency reduced the number of tumor implants in the omentum, abdominal wall and diaphragm (*p≤0.05; ***p≤0.005).*

3. 2 The crosstalk with FGFR signaling underlies multiple functions of L1 in tumor vasculature.

L1 is known to regulate several cellular processes by interacting with and activating signaling receptors. In particular, data previously generated in our lab showed that L1-induced cancer cell migration and invasion are mediated by fibroblast growth factor receptor (FGFR) [104]. Given the pivotal role of FGFR signaling in tumor angiogenesis [115], we hypothesized that L1-induced EC activation might be mediated at least in part by FGFR. We tested this hypothesis in mouse immortalized lung ECs (luECs; [41]). In agreement with previous reports on endothelial cells [116], luEC express only FGFR1, while no detectable expression of FGFR2, FGFR3 and FGFR4 was observed (data not shown).

To test whether FGFR signaling was involved in L1-induced EC processes [41], we performed a series of *in vitro* experiments preventing FGFR activation with the chemical inhibitor PD173074, that was demonstrated to be highly selective for FGFR [117]. The treatment of L1-overexpressing ECs (luEC-L1) with PD173074 reduced significantly L1-dependent endothelial cell proliferation (Figure. 18), migration (Figure. 19) and tube formation (Figure. 20) as compared to control ECs (luEC-mock). This implicated FGFR as a crucial effector in the L1-dependent regulation of key angiogenesis-related events. Our previous data pointed to L1 as a novel regulator of the transcriptional activity in ECs [41]. This raised the possibility that FGFR is involved at least partially in L1-regulated endothelial gene expression. To test this hypothesis, we performed an Affymetrix screening of luEC-L1 and luEC-mock cultured in the presence of PD173074. This analysis, indeed, highlighted a set of genes that were modulated by L1 in vehicle-treated but not in PD173074-treated cells (Figure. 21), pointing to an L1-dependent, FGFR-mediated regulation of gene expression.

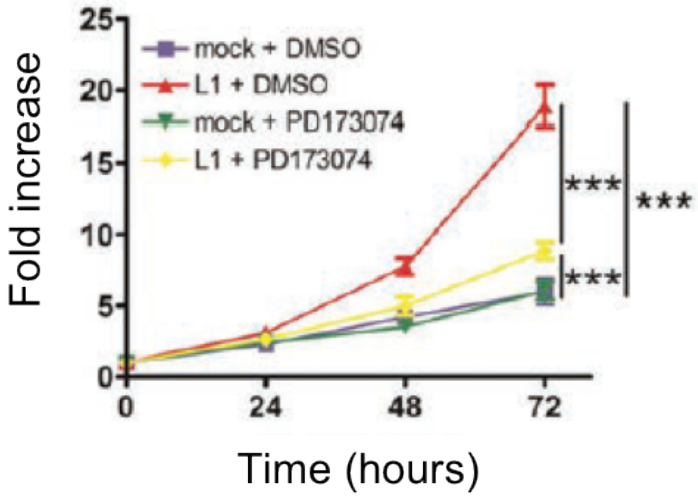

Figure 18. L1-induced EC proliferation required FGFR signaling.

*L1-overexpressing ECs and control cells were cultured in presence of the FGFR inhibitor (PD173074) or vehicle only (DMSO). Curves show the quantitation of EC proliferation at 0, 24, 48 and 72 hours after culturing (*** p <0.005).*

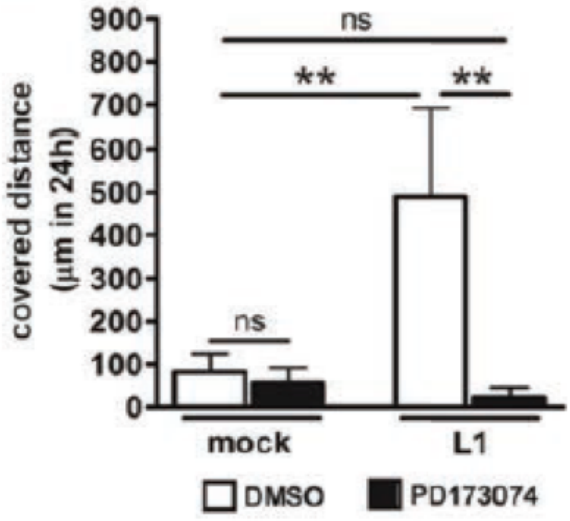

Figure 19. ***L1-induced EC migration required FGFR signaling.***

*Covered distance of migration of mock and L1 transfected luECs in presence of the FGFR inhibitor PD173074 or vehicle only (DMSO) (** p <0.05; ns =not significant).*

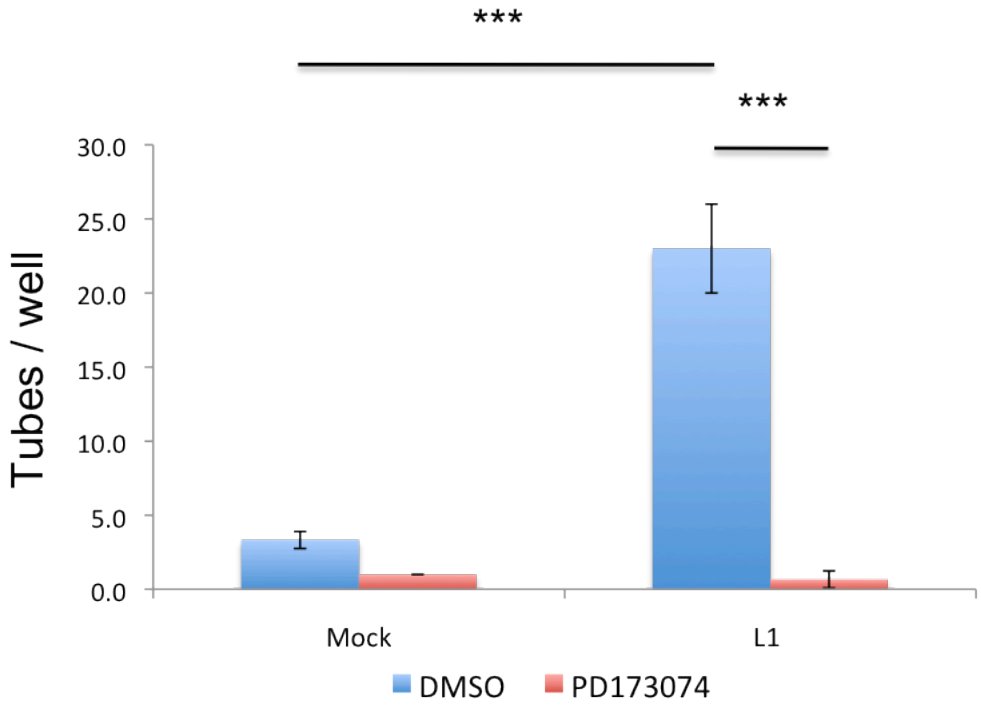

Figure 20. ***L1-induced EC tube-formation required FGFR signaling.***

*Quantitation of tube-formation on mock and L1 transfected luECs in presence of the FGFR inhibitor PD173074 or vehicle only (DMSO) (*** p <0.005).*

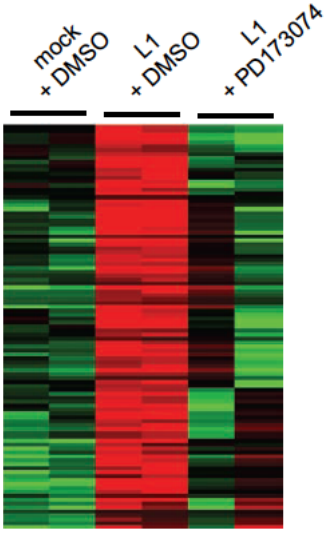

Figure 21. ***L1 regulated a set of genes in FGFR1-dependent manner.***

Heatmap of genes regulated by L1 in luECs which are no longer regulated in the presence of the FGFR inhibitor PD173074. Red, upregulated; green, downregulated.

To validate these data with an alternative and FGFR1-specific approach, we genetically inactivated mouse FGFR1 employing four different shRNAs (sh1, sh2, sh3 and sh4). qRT-PCR analysis confirmed that FGFR1 expression was reduced both in luEC-L1 and luEC-mock by about 70% with sh1 and by about 40% with sh2 and sh4, as compared with a scramble shRNA. Sh3, instead, decreased FGFR1 expression of about 20% in luEC-mock and about 50% in luEC-L1 (Figure. 22).

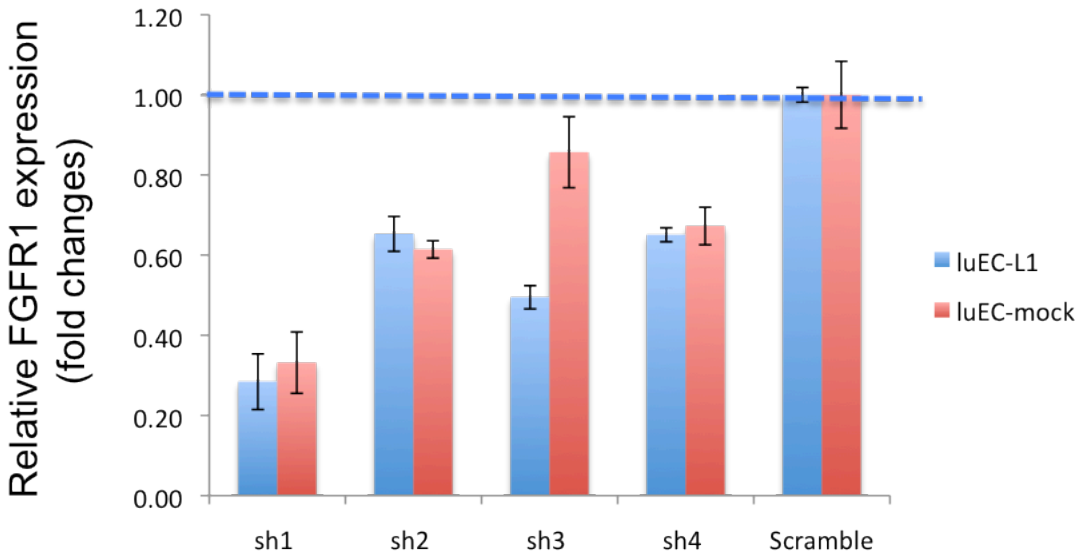

Figure 22 . ***Genetic inactivation of mouse FGFR1 in luECs.***

Mouse FGFR1 was silenced by four different shRNA in luEC-L1 and luEC-mock. After five days of puromycin selection, RNA was extracted from antibiotic-resistant luECs and qRT-PCR was performed to measure the expression of FGFR1. The downregulation of FGFR1 expression by shRNA was statistically significant ($p \leq 0,05$) for all the shRNA as compared to the scramble shRNA (negative control).

Since the sh1 (hereafter referred as sh-FGFR1) showed the highest efficiency in decreasing FGFR1 expression in both luEC-L1 and luEC-mock, we selected this shRNA for further experiments. In order to validate the results obtained with PD173074 chemical inhibitor, FGFR1-silenced luECs were subjected to tube formation assays in matrigel. The down-

modulation of FGFR1 by shRNA impaired L1-dependent capability of endothelial cells to form tube structures (Figure. 23), thus confirming the results obtained with the chemical inhibitor.

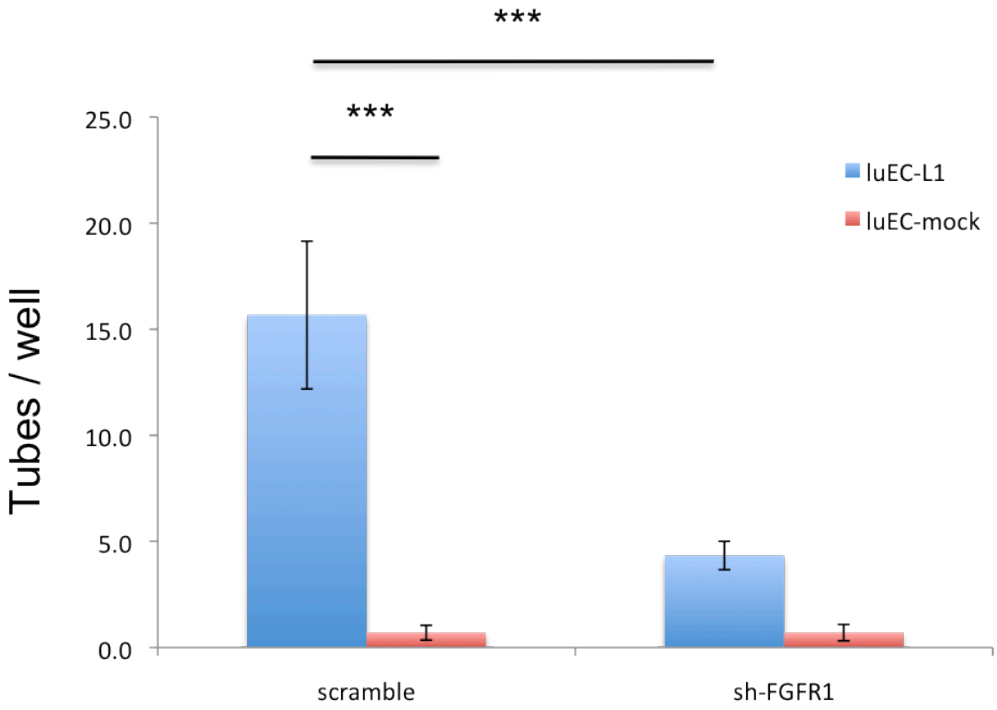

Figure 23. ***L1-induced EC tube formation requires FGFR signaling.***
*After FGFR1 silencing by shRNA, luECs were plated on matrigel-coated wells to form tube like structures. Bars represent the number of tube-like structures formed by mock and L1 transfected luECs after the genetic inactivation of FGFR1 by shRNA. Scramle shRNA was used as negative control (*** $p \leq 0{,}005$).*

We also attempted to validate the PD173074 data on L1-regulated gene expression with shRNA-mediated ablation of FGFR1. To this goal, we performed a quantitative traits analysis of the data obtained from the above mentioned Affimetrix analysis (Figure. 21). Briefly, this tool allows finding genes that correlate significantly with a specified quantitative variable (called trait). In our case it is the L1-induced and FGFR-dependent regulation of genes in endothelium. In our experiment, each gene derived from Affimetrix

analysis that follows the trait was scored with a correlation coefficient and with a p-value. A coefficient higher than 0.7 means that the gene analyzed has a strong correlation with the trait studied. Based on this analysis, we selected the following four genes regulated by L1 in FGFR1-dependent manner: *Egr1*, *Robo4*, *Rab5b* and *Sipa1* (Table 2). These candidates were selected because they were significantly regulated by L1 in a FGFR-dependent manner and because of biological considerations. Indeed, both Robo4 [118,119] and Egr1 [120,121] have been already described as pivotal players in tumor angiogenesis and/or in vessel architecture. Conversely, the involvement of Rab5b and Sipa1 proteins in tumor angiogenesis has been poorly described and their novelty in this field make them particularly appealing for further studying. Our qRT-PCR data confirmed the L1-mediated up-regulation of all the selected candidates (Figure. 24, blue bars). Moreover, upon FGFR1 inactivation by shRNA, the expression of all these genes was significantly reduced (Figure. 24, red bars) confirming that their expression was mediated by FGFR1 in endothelial cells.

Overall, our data highlighted a novel interplay between L1 and FGFR that orchestrates important biological processes in endothelial cells.

Gene name	Gene symbol	Correlation coefficient	p-value
Early growth response 1	*Egr1*	0.879	0.004
RAB5B, member RAS oncogene family	*Rab5b*	0.876	0.004
Roundabout homolog 4 (Drosophila)	*Robo4*	0.87	0.005
Signal-induced proliferation associated gene 1	*Sipa1*	0.912	0.001

Table 2. ***Genes up-regulated by L1 in FGFR1-dependent manner.***
List of *genes selected from Affimetrix analysis performed on luEC-L1 and luEC-mock in the presence of PD173074 or vehicle (DMSO). These genes were up-regulated by L1 and their regulation no longer occurred upon treatment with the FGFR inhibitor PD173074.*

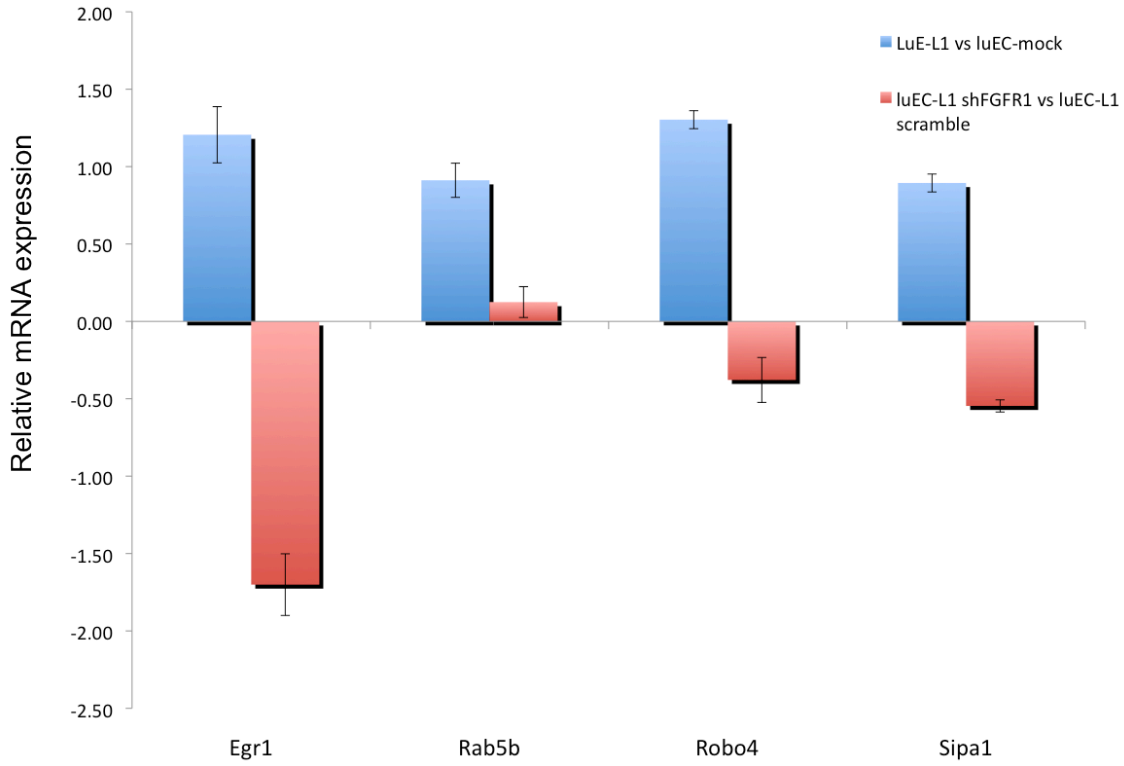

Figure 24. ***qRT-PCR analysis of Egr1, Rab5b, Robo4 and Sipa1 genes in luEC-L1 and luEC-mock after FGFR1 inactivation by shRNA.***

Total RNA was extracted from luEC-L1 and luEC-mock after FGFR1 inactivation by shRNA. The expression of Egr1, Rab5b, Robo4 and Sipa1 genes was evaluated by qRT-PCR. The expression of all genes was induced by L1: blue bars represented the expression of each gene in luEC-L1 as compared to luEC-mock. Upon FGFR1 inactivation, the L1-induced up-regulation all genes was reverted. Red bars represented the expression of these genes in luEC-L1 silenced with sh-FGFR1 normalized to the expression of the same gene in luEC-L1 transduced with scramble shRNA.

3. 3 Vascular L1 regulated the crosstalk between microenvironment and tumor cells: implications for ovarian cancer growth and for cancer stem cell function.

Tumor epithelial cells coexist in carcinomas with several distinct stromal cell types that together create the tumor microenvironment. In the last years, many groups have highlighted the contribution of the microenvironment to the development of a variety of tumors. The accumulated evidence indicates that tumor cells actively recruit stromal cells,

such as inflammatory cells, vascular cells, and fibroblasts [8,122] , into the tumor, and that this recruitment is essential for the generation of a microenvironment that actively fosters tumor growth [123]. In particular, many groups have reported the existence of a signaling crosstalk between tumor cells and ECs that enhance tumor growth in cell contact-dependent [124] as well as independent manner [125].

Based on these considerations as well as on our previous data that showed reduced tumor growth upon endothelial ablation of L1 [41], we asked whether vascular L1 modulates ovarian cancer growth. To this end, GFP-expressing ID8 cells were co-injected subcutaneously into immunodeficient NOD/SCID/IL2Rg^{null} mice with either luEC-L1 or luEC-mock. We tested two different ID8:luEC ratios, 1:1 and 5:1. As soon as 8 (1:1 ratio) or 15 days (5:1 ratio), all transplanted mice showed the formation of hemangioma-like structures (Figure. 25 and 26), reflecting the fact that ECs overgrew ID8 cells. This result was most likely due to the combination of two factors: the immortalization of luECs with polyoma middle-T-antigen which indeed might underlie hemangiomas *in vivo* [41,109] and the relatively slow growth rate of ID8 cells when transplanted subcutaneously [126,127]. Nevertheless, we undertook this co-transplantation approach to assess whether L1-overexpressing endothelial cells exerted a sort of "priming" effect on ID8 cells. To this goal, first-generation tumors (consisting of small ID8 masses plus luEC-derived hemangiomas) were enzymatically digested and GFP-expressing ID8 cells were purified from cell suspension by FACS-sorting. Then, ID8 cells were re-transplanted alone into NOD/SCID/IL2Rg^{null} mice to form second-generation tumors. Notably, ID8 cells derived from the co-transplantation with luEC-L1 were more tumorigenic as compared with control cells (Figure. 27), suggesting that L1-expressing EC had somehow "primed" OC cells enhancing their tumorigenic activity.

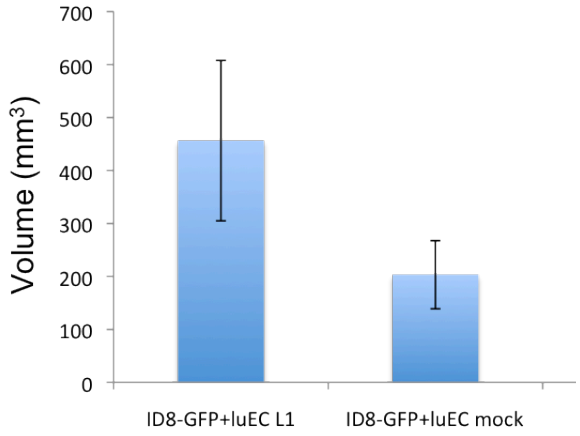

Figure 25. ***Co-transplantation of ECs and ID8 cells resulted in the formation of hemangioma-like structures.***

GFP-expressing ID8 cells were injected subcutaneously into NOD/SCID/IL2Rg^{null} mice admixed with luEC-L1 or luEC-mock (1:1 ratio); bars indicate the volume of hemangiomas (n=5) at the endpoint of the experiment.

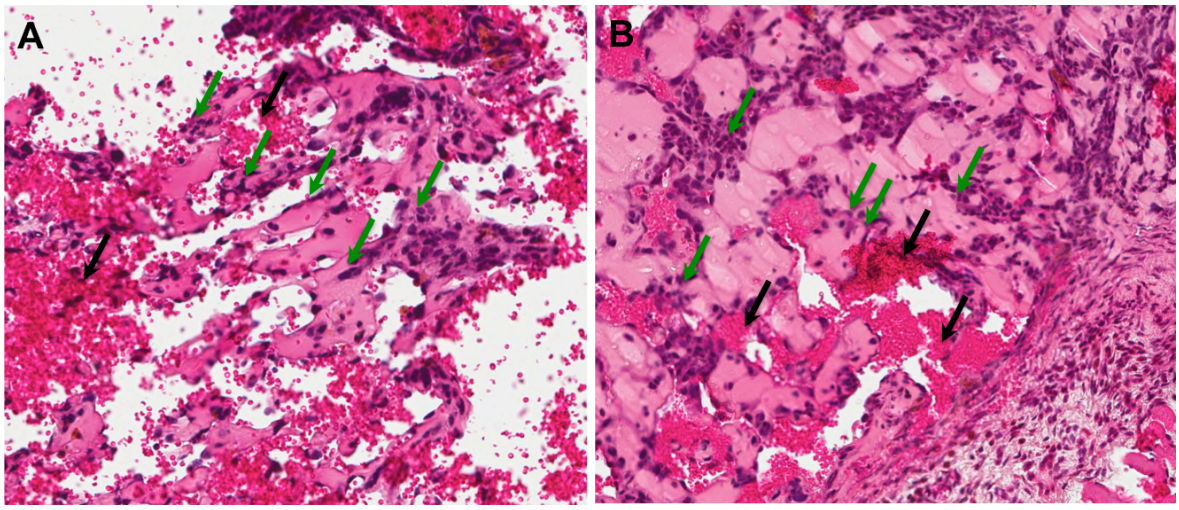

Figure 26. ***ID8 cells mixed with luECs developed hemangioma-like structure in immunocompromised mice.***

H&E staining of tissue section from hemangiomas lesions derived from ID8 cells transplanted subcutaneously together with luEC-L1 (A) or luEC-mock (B) in NOD/SCID/IL2Rg^{null} mice (n=5). These representative images highlighted two typical characteristics of haemangioma: the presense of newly formed vessels (green arrows) and the accumulation of red blood cells (black arrows).

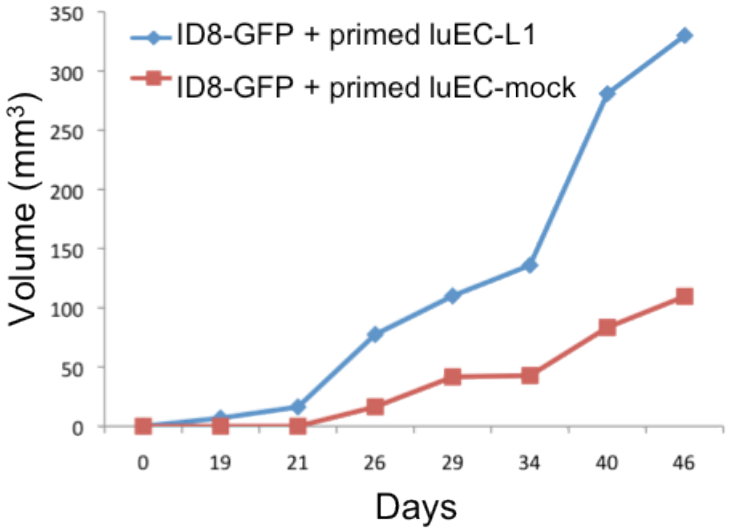

Figure 27. ***Serial transplantation of ID8 cells primed by L1-overexpresing luECs showed enhanced tumorigenicity.***

GFP-expressing ID8 cells mixed with luECs were transplanted subcutaneously in NOD/SCID/IL2Rg^{null} mice. After enzymatic digestion of tumors, GFP expressing ID8 cells were purified by FACS-sorting and retransplanted into mice at 2x10^{4} cells/mouse (n=2). Curves show the kinetic of tumor growth of ID8 cells primed with luEC-L1 (blue) or luEC-mock (red).

To determine if the direct cell-cell contact was required for such a pro-tumorigenic effect of L1-overexpressing luECs, we performed a similar experiment but this time using conditioned medium (CM) collected from luEC-L1 or from luEC-mock. In particular, NOD/SCID/IL-2 Rg^{null} mice were transplanted with ID8 cells admixed with either luEC-L1- or luEC-mock-derived CM (our control). Interestingly, luEC-L1-derived CM was sufficient to enhance OC growth while luEC-mock-derived CM had no effect (Figure. 28), suggesting that vascular L1 is able to modulate tumor growth also in cell-contact independent manner.

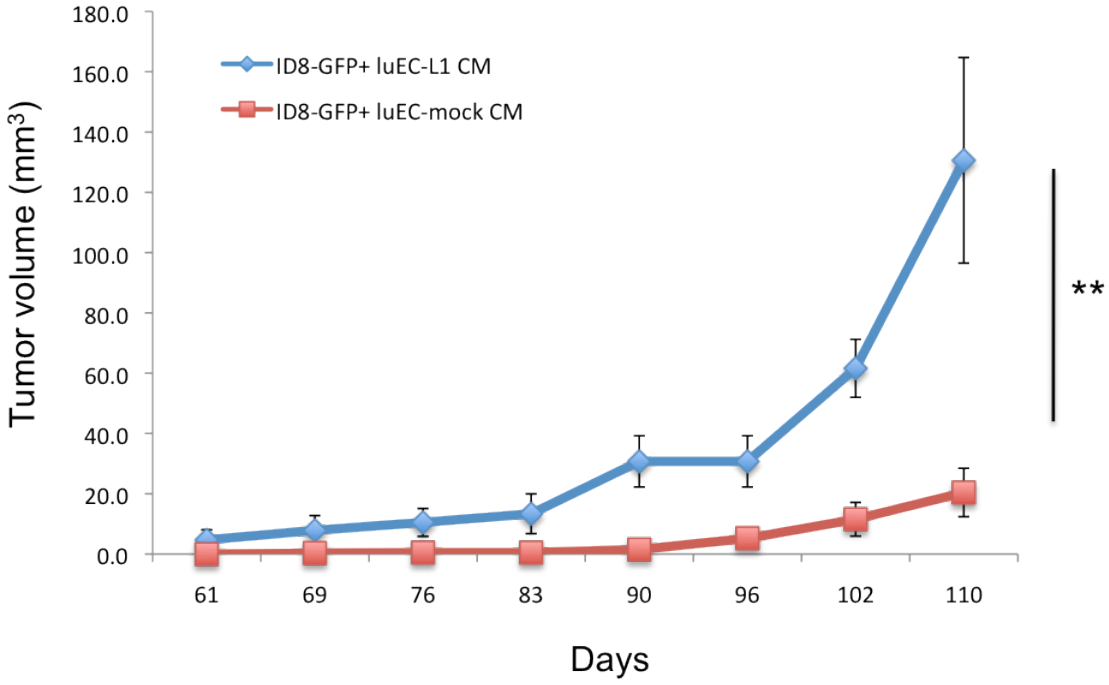

Figure 28. ***LuEC-L1-derived CM promoted OC growth in vivo.***

*GFP-expressing ID8 cells were injected subcutaneously into NOD/SCID/IL2Rg^{null} mice (n=10), alone or admixed with CM from luEC-L1 or from luEC-mock, and tumor growth was monitored. ID8 cells co-transplanted with luEC-L1-derived CM formed tumors with a higher growth rate than cells co-transplanted with luEC-mock-derived CM (** p<0.05).*

The capability of either luEC-L1 cells or luEC-L1-derived CM to foster tumor formation might be associated with the acquisition by tumor cells of markers associated with epithelial-mesenchymal transition (EMT). The latter, indeed, is a hallmark of cancer progression, and the expression of EMT related markers correlates with a more aggressive behavior of tumor cells and eventually with an increased metastatic potential [128,129]. Of note, we have already demonstrated that L1 induces the expression of EMT-related genes [41]. For all these reasons, we analyzed EMT markers in tumors derived from ID8 cells mixed with luEC-L1- or luEC-mock-derived CM. A preliminary analysis of a panel of EMT-related genes on tumor samples revealed that luEC-L1-derived CM induced the expression of the EMT-related genes *Cdh2, Vim, Zeb1, Zeb2, Snail1, Twist* and *Klf4* while it caused the down-regulation of the epithelial marker *Krt8* (Figure. 29), indicating that L1-dependent induction of EMT occurs *in vivo*.

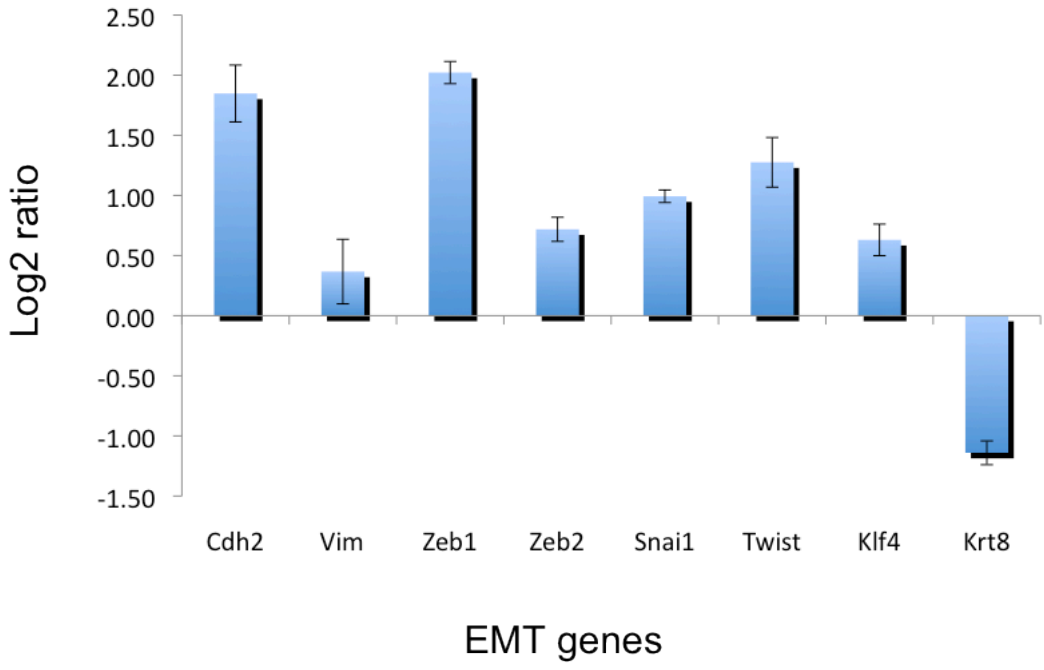

Figure 29. ***LuEC-L1-derived CM induced the expression of EMT-related genes in vivo.*** *Total RNA was extracted from paraffin-embedded tumors derived from ID8 cells admixed either with luEC-L1- or luEC-mock-derived CM (n=2). EMT-related genes were analyzed by qRT-PCR. Bars represent the level of expression of EMT-related genes. luEC-L1-derived CM induced the expression of a series of EMT-genes and it determined the down-regulation of the epithelial marker Krt8.*

Besides supporting tumor cell invasion, EMT correlates with the acquisition of cancer-initiating properties by tumor cells. Indeed, the expression of EMT genes is frequently accompanied by the expression of genes related to tumor-initiating cells or CSCs [42,130]. In agreement with this notion, we noticed that ID8 cells primed with luEC-L1 formed tumors that were already palpable after 19 days post-injection, while tumors from ID8 cells primed with luEC-mock became palpable after 26 days (Figure. 30). The latency of ID8 cells exposed to luEC-L1-derived CM was also significantly shorter than that of cells co-transplanted with luEC-mock-derived CM (Table. 3), implying that the direct contact of L1-expressing ECs with tumor cells is dispensable for the effect on tumor initiation.

Overall these data showed that vascular L1 decreases OC tumor latency and promotes

tumorigenesis, concomitant to the induction of EMT. Our finding highlighted the pivotal role of L1 in microenvironment-regulated OC growth.

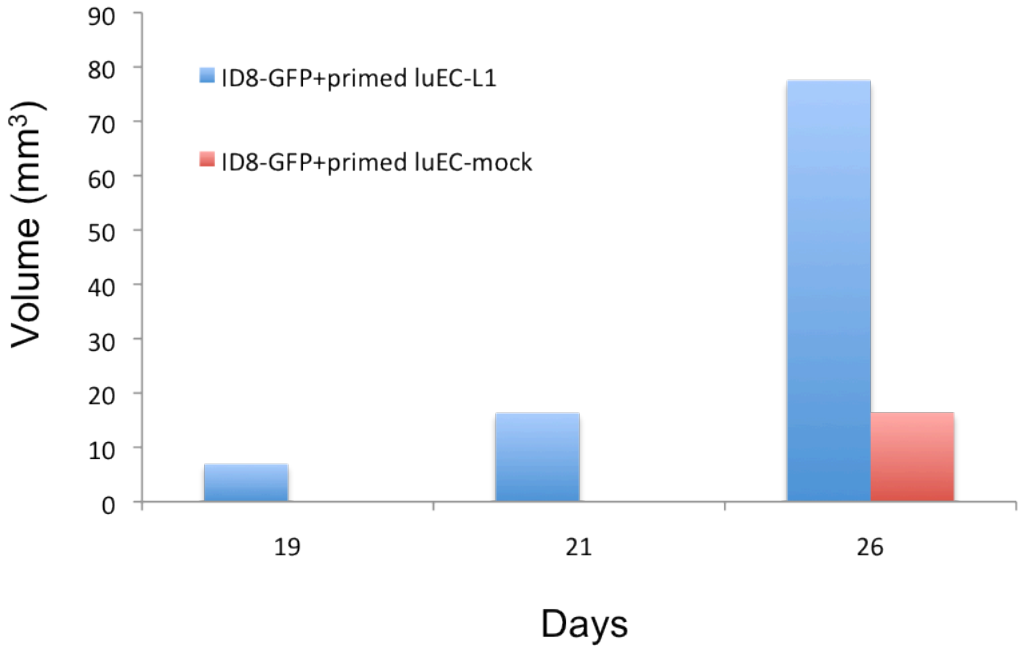

Figure 30. ***ID8 cells primed with L1-overexpressing luEC cells showed a decreased latency in mice.***

GFP-expressing ID8 cells mixed with luECs were transplanted subcutaneously in NOD/SCID/IL2Rg^{null} mice. After enzymatic digestion of tumors, GFP expressing ID8 cells were purified by FACS-sorting and retransplanted into mice at 2x10^{4} cells/mouse (n=2). Bars show a reduction in the latency of ID8 tumors. While ID8 cells primed with luEC-L1 formed tumors by 19 days after transplantation (blu bar), ID8 cells primed with luEC-mock became visible 7 days after (red bar).

	Mice with tumor			
Days after injection	40	61	69	76
ID8 + luEC-L1-derived CM	0/10	7/10	10/10	10/10
ID8 + luEC-mock-derived CM	0/10	0/10	2/10	3/10

Table 3. ***LuEC-L1 derived CM decreased ID8 tumor latency in mice.***
GFP-expressing ID8 cells were mixed with CM derived from luEC-L1 or luEC-mock and were transplanted subcutaneously in NOD/SCID/IL2Rg^{null} mice (n=10). While ID8 cells mixed with luEC-L1 derived CM formed tumors by 61 days after transplantation, ID8 cells mixed with luEC-mock derived CM became visible 69 days after the beginning of the experiment.

3. 4 Vascular L1 induced stemness in OC cells

An increasing body of evidence supports the notion that tumor initiation is accounted for by the sub-population of the so-called tumor-initiating cells or CSCs. These cells often reside in specialized microenvironment, which are localized in the close proximity of tumor vessel, called perivascular niches, where a cross-talk with endothelial cells is crucial for their survival [47]. Since our *in vivo* experiment showed that luEC-L1-derived CM promoted tumor initiation, to verify whether vascular L1 promotes ovarian CSC (OCSC) function, we performed a sphere formation assays. This is a widely used technique for determining CSC frequency in a cell population and it is an indirect measure of inherent stemness-associated biological properties [131]. In particular, we cultured a low number of ID8 cells under non-adherent conditions to form monoclonal spheroids, in the presence of either luEC-L1- or luEC-mock-derived CM. The addition to the culture of luEC-L1-derived CM enhanced the percentage of ID8 cells able to form spheres (Figure. 31) as compared with luEC-mock-derived CM or ID8 cells cultured in absence of CM ("no CM"), supporting a role of vascular L1 in promoting the OCSC phenotype.

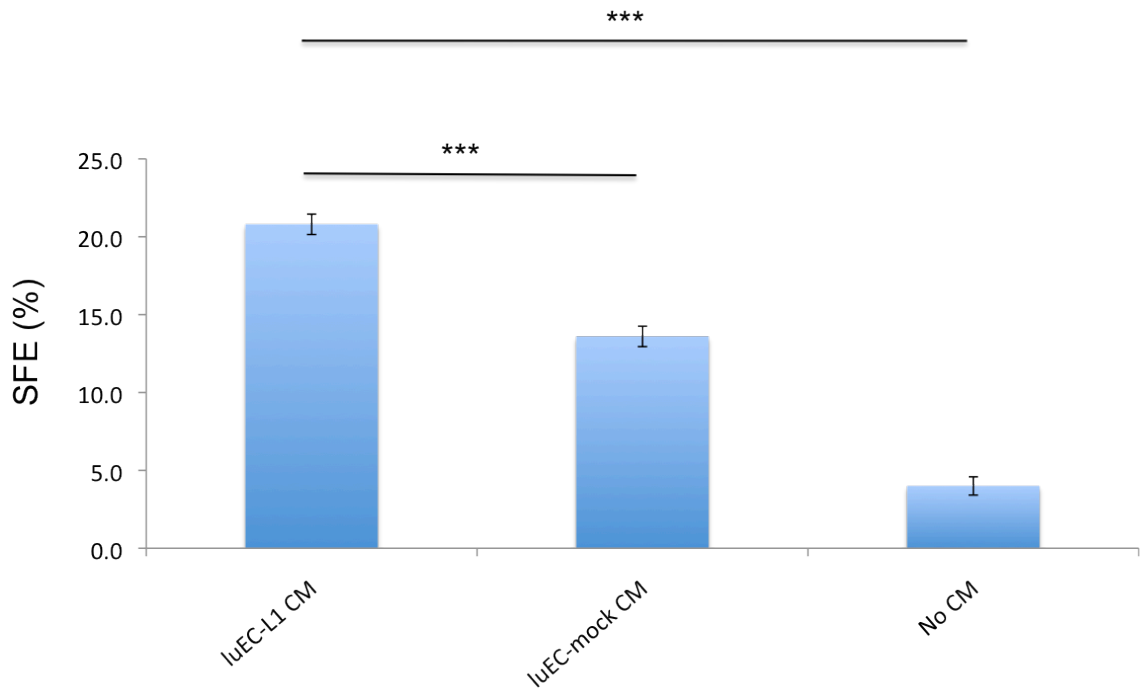

Figure 31. ***LuEC-L1-derived CM increased the capability of ID8 cells to growth as spheres.***

*ID8 cells were cultured under non-adherent conditions at very low concentration (500 cells/ml) in the presence of CM from luEC-L1 or luEC-mock (or no CM). After 5 days, clonal spheres were counted and the sphere-forming efficiency (SFE) was determined as the percentage of cells from the original cultures able to form spheres. The addition of 1/3 of luEC-L1-derived CM to the culture increased the SFE of ID8 cells as compared to CM from luEC-mock or to medium without CM (*** $p<0.005$).*

Our data showed that CM derived from L1-overexpressing luECs is able to promote CSC-related properties to OC cells *in vitro* and *in vivo,* as shown by sphere formation and tumor initiation data. In an attempt to identify the molecule(s) able to confer this phenotype to OC cells, we took advantage of results recently published from our lab where we showed that luEC-L1 secrete IL-6 in conditioned medium derived from endothelial cells [41]. IL-6 has a critical role in promoting a cancer stem cell-phenotype in several neoplasms such as breast and brain tumors [132,133], thus implying that this molecule may act downstream of vascular L1 to promote ovarian tumor initiation and cancer growth. To test whether vascular IL-6 mediates the L1-induced acquisition of OCSC traits, ID8 cells were

subjected to sphere formation assays in the presence of luEC-L1-derived CM previously depleted of IL-6 by immunoprecipitation. IL-6 depletion abolished the sphere-forming capability induced by luEC-L1-derived CM, demonstrating that this secreted molecule has a critical role as an L1 effector in promoting CSC phenotype (Figure. 32).

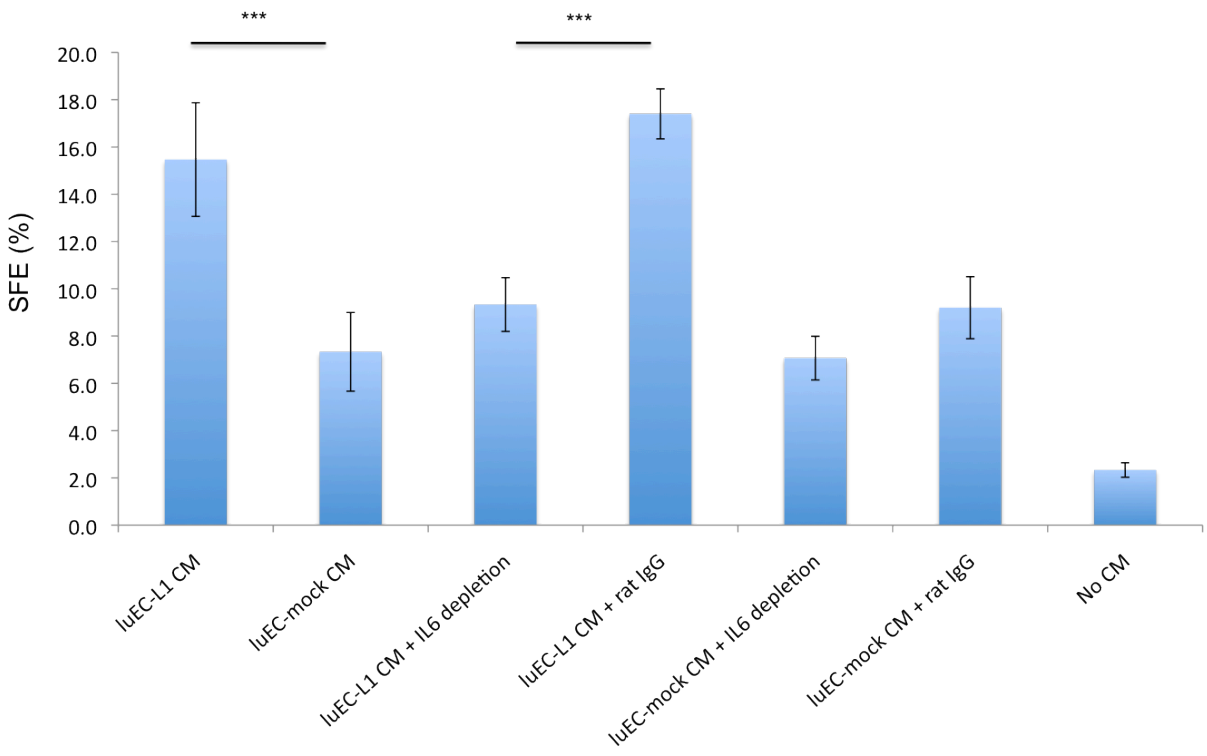

Figure 32. ***IL-6 mediates L1-induced sphere forming ability in ID8.***

*ID8 cells were cultured under non-adherent conditions at very low concentration (500 cells/ml) in the presence of CM from luEC-L1 or luEC-mock (or no CM) depleted from IL-6 by immunoprecipitation. After 5 days, clonal spheres were counted and the sphere-forming efficiency (SFE) was determined as the percentage of cells from the original cultures able to form spheres. The depletion of vascular IL-6 from luEC-L1-derived CM reduced nearly by 50% the SFE of ID8 cells as compared to luEC-L1 derived CM (*** $p<0.005$).*

4 DISCUSSION

The expression of L1 in tumor-associated vasculature has been reported for several tumor types, including breast, ovarian and pancreatic carcinoma [100,108]. Our group has also demonstrated that L1 plays a functional role in tumor vasculature. Indeed, endothelial L1 deficiency results in reduced tumor growth and tumor angiogenesis, while it promotes vascular normalization. Moreover, the treatment of tumor-bearing mice with a polyclonal anti-L1 antibody mimics the genetic inactivation of L1 [41], thus pointing to L1 not only as a marker of pathological angiogenesis but also as a novel potential target for anti-angiogenic therapy.

Based on these findings, one of the main objectives of my project was to test whether vascular L1 is involved also in OC malignancy. In this context, a deeper understanding of the molecular mechanisms that drive vessel pathophysiology in OC is likely to have important implications, given that the vascular system plays a pivotal role in OC and the addition of VEGF-based anti-angiogenic drugs to standard chemotherapy gave promising results in clinics [77].

Using a syngeneic orthothopic model of OC based on the ID8 ovarian cancer cell line we have demonstrated that vascular L1 deficiency reduced the tumorigenicity and the dissemination of ID8 ovarian cancer cells in the abdominal wall, in the omentum and in the diaphragm of mice, typical sites of OC spreading also in patients. These results suggest that the expression of L1 in tumor vasculature offers a growth advantage for ID8-derived tumor implants. Indeed, it is plausible that OC cells adhere to several organs in the abdominal cavity of mice but that their growth up to measurable tumor lesions requires L1-mediated angiogenesis.

The clinical relevance and the possible translational application of our *in vivo* results were supported by the immunohistochemical analysis of vascular L1 expression in human OC

versus its normal counterpart. Interestingly, L1 is expressed in 80% of vessels in OC samples while only 20% of vessels expressed L1 in normal ovaries.

The results obtained in OC mouse model together with the immunohistochemical analysis performed on human samples pointed to L1 as a potential target in the context of pathological angiogenesis. Notably, even if the VEGF- based anti-angiogenic therapy gave promising results in OC patients, the appearance of cancers able to resist/escape to therapy represents one of the main limits to the use of such drugs in clinics [35]. Therefore, the identification of new vascular mechanisms and targets is an urgent need, and L1 might represent a suitable candidate to develop innovative anti-angiogenic drug and overcome the current limitations of anti-angiogenic therapy. Moreover, its expression at the cell surface together with its abundance in tumor vasculature (as compared with the normal counterpart), make L1 particularly appealing for further studying and drug development.

Another important aspect of L1 function in endothelium is its involvement in vessel architecture [41]. L1-expressing vasculature showed abnormal polarity, loss of VE-cadherin-mediated endothelial junction and increased permeability. As a consequence, vascular L1 deficiency resulted in decreased vessel permeability and vascular normalization [41]. Although the concept of "*vascular normalization*" and its therapeutic significance are very debated in the field [11], both preclinical [29] and clinical studies [32,34] have provided evidences of improved vascular maturation and stability upon treatment with anti-angiogenic drugs.

Furthermore, the existence of a "*normalization window*", as a consequence of anti-angiogenic treatment, might help in solving the apparent paradox represented by the fact that anti-angiogenic agents boost the efficacy of chemotherapy [134]. Indeed, several studies have showed an increase in chemotherapeutics uptake within the tumor after anti-angiogenic treatment [135,136]. In other cases, although the concentration of chemotherapeutics in the tumor mass decreased upon anti-angiogenic treatment [137,138], it is associated with a slower efflux of these agents from the tumor, thus prolonging the time of

contact between tumor cells and drugs. Moreover, independently from the amount of drug able to reach the tumor, a normalized vasculature results in a more homogeneous intratumoral distribution of anticancer therapies [137]. These findings in preclinical model might help explaining also the results obtained in recent clinical trials in OC patients, in which the addition of Bevacizumab to standard chemotherapy increased the PFS as compared to treatment with chemotherapy only.

In this context, the simultaneous administration of an L1 inhibitor as anti-angiogenic and vascular-normalizing agent together with standard chemotherapy might result in a synergistic effect with significant clinical benefit for OC patients. Of course, the toxicity related to inhibiting L1 remains an issue that needs to be addressed, however, earlier reports on preclinical models [41,105,107] support the feasibility. For example, the treatment of tumor-bearing mice with a polyclonal anti-L1 antibody showed no significant side effects [41] while it determined a reduction in tumor angiogenesis, tumor growth and metastasis [41], supporting the potential translational application of these findings.

These *in vivo* findings were supported by several experiments performed *in vitro*, using luECs. The main objective of this part of this work was to further characterize the molecular mechanisms underling the multiple function of L1 in endothelium [41]. We have previously demonstrated that the up-regulation of L1 in ECs induced cell migration, proliferation and tube formation [41]. Moreover, the ectopic expression of L1 in ECs determined the regulation of genes involved in angiogenesis, EMT and cell proliferation [41]. However how this cell adhesion molecule modulates all these process in endothelium remain elusive.

Based on the notion that L1-induced cancer cell migration and invasion are mediated by fibroblast growth factor receptor (FGFR) [104] and that the FGF/FGFR signaling pathway

plays a pivotal role in angiogenesis [115], we investigated a possible relationship between L1 and FGFR in endothelium. These experiments revealed the involvement of FGFR in L1-dependent regulation of endothelial cell proliferation, migration and tube formation. Although we have not investigated the molecular basis of such interplay between FGFR and L1, a possible mechanism might be represented by a direct interaction between vascular L1 and FGFR. This hypothesis is supported by the fact that L1 engages in heterophilic interactions with RTKs and that a direct binding of L1 to FGFR1 has been already demonstrated [139,140]. In endothelial cells, surface-bound L1 could stimulate FGFR activation by *cis* interaction as well as by *trans* interactions upon cell-cell contact. Alternatively, it has been established that L1 can undergo proteolytic cleavage that results in the shedding of its biologically active ectodomain [94,96,141]. The latter could act as a soluble ligand for FGFR, thus promoting endothelial cell proliferation, migration and tube formation. Another key aspect that future studies should address is whether L1 exerts a direct and autonomous role on FGFR activation or it rather modulates the response of the receptor to its classical ligand, FGF. In this context, our group has previously demonstrated that the L1-related molecule NCAM not only acts as a direct activating ligand for FGFR eliciting a response that is divergent from that elicited by FGF [142], but it also negatively regulates the binding and the biological activity of FGF itself [143]. On the other hand it is also conceivable that L1 acts in a synergistic manner with FGF, for example by preventing the rapid internalization and degradation of FGFR upon ligand binding, thus resulting in sustained signaling and endothelial cell activation.

The broad spectrum of FGFR-mediated biological processes induced by L1 in endothelial cells is consistent with the large series of genes that are modulated by L1 via FGFR, which implies a massive influence of this crosstalk on gene transcription. Based on these considerations and on the well established pro-angiogenic role of FGF/FGFR signaling pathway in tumor angiogenesis and the aberrant phenotype correlated with L1-expression in tumor vasculature, a deeper understanding of their molecular interplay and/or their

integrated regulation of other signaling pathways, might be an important step for the design of novel anti-angiogenic therapy. Indeed, it is already known that FGFR signaling cascade is activated to compensate the VEGF-deprivation upon VEGF-based anti-angiogenic therapy [35]. Moreover, anti-FGF/FGFR compounds are already used in clinics, even if with non-negligible side effects [144]. The simultaneous block of L1 and FGFR might represent a novel and more effective anti-angiogenic therapy to treat OC patients. Moreover, the use of a putative anti-L1 drug might result in the indirect blocking of several genes/pathways expressed and/or regulated by FGFR activation and it might represent a strategy to overcome the toxicity of FGFR inhibitors.

Another intriguing function of ECs in tumors is represented by their active role in fostering tumor growth. In this view, ECs not only provide tumor with the physical structure to allow blood flow but they also express/secrete molecules able to promote cancer growth. Indeed, several studies have highlighted the existence of a signaling crosstalk between tumor cells and ECs that actively promotes tumor growth [124]. Notably, our data indicate that vascular L1 promotes OC growth *in vivo.* Indeed, the serial transplantation of ID8 OC cells "primed" with luEC-L1 showed an enhanced tumorigenicity as compared with the same cells co-transplanted with control ECs. Moreover, we have demonstrated that the cell-cell contact is dispensable for the pro-tumoral effect of L1-overexpressing luECs. Indeed, luEC-L1-derived CM is effective in promoting OC growth, suggesting a pro-tumoral role of factor(s) secreted by L1-overexpressing endothelial cells. These data indicate a role of vascular L1 in fostering OC growth, thus contributing to define a novel interplay between microenvironment and tumor cells.

It has long been known, also based on data from our lab, that L1 is highly expressed in cancer cells, including OC cells [104]. It is conceivable that tumor-derived L1 acts as a pro-angiogenic molecule by stimulating EC activation in a paracrine manner. For example, L1

expressed in OC cancer cells might induce the activation of FGFR in adjacent vessels. In this context, the proteolyitc cleavage of the extracellular domain of L1 [92] and the consequent release of its soluble form that retains biological activity [96] might reflect the ability of tumor cells to generate an L1-derived angiogenic ligand. A further layer of complexity to such an intercellular signaling might come from the co-expression of L1 in both cancer cells and vascular endothelium. This might promote homophylic L1-L1 interactions which would likely have a profound impact on the resulting signal. For example, since *trans* L1 binding promotes clustering of the molecule on the cell surface, in the case of FGFR these interaction might lead to FGFR clustering and, therefore, to amplification of the angiogenic signal. Overall, this hypothesis supports an active role of tumor-derived L1 (both surface-bound and/or soluble) in tumor angiogenesis.

Taken together with our present results, these considerations support the existence of a bidirectional crosstalk between ECs and tumor cells in which the two cell types modulate each other through L1-mediated signaling. In this scenario, a putative L1-based anti-angiogenic therapy might have multiple effect, blocking both the cell-autonomous role of L1 in tumor vasculature on one hand and in cancer cell on the other, as well as interfering with the signaling crosstalk between the two cell types.

The enhanced tumorigenicity of luEC-L1-derived CM seems to be, at least in part, associated with the acquisition of EMT-related markers. Although the qRT-PCR analysis for EMT-associated genes was performed in a very limited set of samples, it revealed that luEC-L1-derived CM promoted the up-regulation of Cdh2, Zeb1, Zeb2, Snail1, Twist and Klf4 together with the loss of the epithelial marker Krt8. The role of L1 in EMT has been clearly established in various experimental models, especially in cancer cells [102,145]. However, those studies have documented a cell-autonomous function, whereby the expression of L1 per se promoted EMT [146]. Our results provide an additional mechanism in

which EMT in cancer cells is regulated by vessel-derived L1 in a paracrine manner through secreted factors. Future studies should aim at identifying the factors themselves, in particular clarifying whether EMT is directly induced by the extracellular domain of L1 released by ECs in the surrounding environment or rather by molecules that are secreted by ECs in a L1-dependent manner.

The EMT process, besides conferring invasive capabilities, is very often intimately linked with the acquisition by tumor cells of cancer-initiating properties or cancer stem-like cells phenotype [42]. The latter hallmarks normally result in shorter tumor latency, which is what we observed upon L1 expression in ECs. Indeed, ID8 cells "primed" by the previous co-transplantation with luEC-L1 or exposed to luEC-L1-derived CM showed a reduction in tumor latency as compared with ID8 primed with control cells or exposed to CM derived from control cells. While these data support the effect of vascular L1 on tumor initiation, the underlying mechanisms remain elusive. Some insights in this regard may come from the different results of my two *in vivo* approaches. Indeed, the re-transplantation of ID8 cells in mice after priming *in vivo* with luEC-L1 resulted in tumor formation by 19 days after injection, while the pro-tumoral effects mediated by luEC-L1-derived CM became visible 60 day after transplantation. This apparent discrepancy in tumor latency might be accounted for by the intrinsic difference between the two experimental procedures. Indeed, when ID8 cells are co-transplanted with endothelial cells, they are exposed for several days to vessel-derived molecules (including L1 itself), both via cell-cell contact and through secreted factors. The high impact of this "priming" phenomenon is also demonstrated by the fact that the number of ID8 cells required for tumor formation was significantly lower in the subsequent transplantation ($2x10^4$) as compared to the number in the initial injection ($1x10^6$), indicating a much higher tumor-initiating ability. In contrast to the long-term exposure of ID8 cells to luEC-L1 during the priming period, cells transplanted with luEC-

L1-derived CM are likely exposed to EC-derived factor for limited time (also due to the short half-life of the factors themselves), thus accounting for longer latency. Consistent with the decreased tumor latency *in vivo*, luEC-L1-derived CM increased the capability of ID8 cells to form spheres *in vitro*, further supporting the notion that factors secreted by EC under the control of L1 promote OC stemness.

Overall, these considerations point to L1 as a novel player in the so-called perivascular niche, namely the specialized microenvironment where CSCs reside and receive survival and proliferation signals from ECs. In the last few years, several groups have focused on the characterization of CSC niches and on the possibility to target the EC/CSC interactions that occur there [47]. Our data suggest that L1 inhibition might contribute to achieve this objective.

Given that endothelial cells release a plethora of molecules in the extracellular environment, a challenging part of this work was the identification of the soluble factor(s) that might account, at least to some extent, for the promotion of OCSC traits. In this context, we reported that L1 induces the expression and secretion of IL-6 by luEC [41], and IL-6 represented a good candidate since it promotes the CSC phenotype in several tumor types [132,133]. Indeed, the depletion of IL-6 from luEC-L1-derived CM abolished its ability to promote ID8 sphere formation, demonstrating that this molecule secreted by ECs plays a critical role in determining CSC traits also in OC.

The novel role of vascular L1 in orchestrating the OCSCs features strengthens the rationale for testing L1 as a target to develop innovative therapies. Indeed, the neutralization of vascular L1 might have a synergistic effect blocking tumor-associated angiogenesis and at the same time preventing the persistence of CSCs in patients after chemotherapeutic treatment. Indeed, one of the factors that might account for tumor relapse in OC patients is the resistance of this subpopulation of cells to the standard chemotherapy, due to their slow dividing rate and their ability to actively pump out such drugs [44].

In summary, my work has demonstrated:

- a functional role of L1 in OC-associated vasculature;
- a crosstalk between L1 and FGFR in endothelial cells;
- a critical role of vascular L1 in promoting the selection/maintenance of OC initiating cells *in vivo*;
- the ability of the secreted molecule IL-6 to act as a vascular L1 effector in promoting OCSC features.

Collectively, this research might pave the way for exploring the clinical relevance of L1 expression and function in OC vessels and its crosstalk with tumor cells, possibly opening new avenues for the development of novel targeted therapies for OC malignancy.

REFERENCES

1 Swift, M. R. & Weinstein, B. M. Arterial-venous specification during development. *Circ Res* **104**, 576-588, doi:10.1161/CIRCRESAHA.108.188805 (2009).

2 Adams, R. H. & Alitalo, K. Molecular regulation of angiogenesis and lymphangiogenesis. *Nat Rev Mol Cell Biol* **8**, 464-478, doi:10.1038/nrm2183 (2007).

3 Takuwa, Y. *et al.* Roles of sphingosine-1-phosphate signaling in angiogenesis. *World J Biol Chem* **1**, 298-306, doi:10.4331/wjbc.v1.i10.298 (2010).

4 Jain, R. K. Molecular regulation of vessel maturation. *Nat Med* **9**, 685-693, doi:10.1038/nm0603-685 (2003).

5 Carmeliet, P. Angiogenesis in life, disease and medicine. *Nature* **438**, 932-936, doi:10.1038/nature04478 (2005).

6 Folkman, J. Tumor angiogenesis: therapeutic implications. *N Engl J Med* **285**, 1182-1186, doi:10.1056/NEJM197111182852108 (1971).

7 Hanahan, D. & Coussens, L. M. Accessories to the crime: functions of cells recruited to the tumor microenvironment. *Cancer Cell* **21**, 309-322, doi:10.1016/j.ccr.2012.02.022 (2012).

8 Ziyad, S. & Iruela-Arispe, M. L. Molecular mechanisms of tumor angiogenesis. *Genes Cancer* **2**, 1085-1096, doi:10.1177/1947601911432334 (2011).

9 Giuliano, S. & Pages, G. Mechanisms of resistance to anti-angiogenesis therapies. *Biochimie* **95**, 1110-1119, doi:10.1016/j.biochi.2013.03.002 (2013).

10 Dejana, E., Tournier-Lasserve, E. & Weinstein, B. M. The control of vascular integrity by endothelial cell junctions: molecular basis and pathological implications. *Dev Cell* **16**, 209-221, doi:10.1016/j.devcel.2009.01.004 (2009).

11 Carmeliet, P. & Jain, R. K. Principles and mechanisms of vessel normalization for cancer and other angiogenic diseases. *Nat Rev Drug Discov* **10**, 417-427, doi:10.1038/nrd3455 (2011).

12 Jain, R. K. Normalization of tumor vasculature: an emerging concept in antiangiogenic therapy. *Science* **307**, 58-62, doi:10.1126/science.1104819 (2005).

13 Carmeliet, P. & Jain, R. K. Angiogenesis in cancer and other diseases. *Nature* **407**, 249-257, doi:10.1038/35025220 (2000).

14 Jain, R. K. Normalizing tumor vasculature with anti-angiogenic therapy: a new paradigm for combination therapy. *Nat Med* **7**, 987-989, doi:10.1038/nm0901-987 (2001).

15 McDonald, D. M. & Choyke, P. L. Imaging of angiogenesis: from microscope to clinic. *Nat Med* **9**, 713-725, doi:10.1038/nm0603-713 (2003).

16 Leung, D. W., Cachianes, G., Kuang, W. J., Goeddel, D. V. & Ferrara, N. Vascular endothelial growth factor is a secreted angiogenic mitogen. *Science* **246**, 1306-1309 (1989).

17 Senger, D. R. *et al.* Tumor cells secrete a vascular permeability factor that promotes accumulation of ascites fluid. *Science* **219**, 983-985 (1983).

18 Potente, M., Gerhardt, H. & Carmeliet, P. Basic and therapeutic aspects of angiogenesis. *Cell* **146**, 873-887, doi:10.1016/j.cell.2011.08.039 (2011).

19 Ruscito, I. *et al.* Cediranib in ovarian cancer: state of the art and future perspectives. *Tumour Biol* **37**, 2833-2839, doi:10.1007/s13277-015-4781-4 (2016).

20 Zhao, H. *et al.* Pazopanib diminishes non-small cell lung cancer (NSCLC) growth and metastases in vivo. *Thorac Cancer* **6**, 133-140, doi:10.1111/1759-7714.12138 (2015).

21 Kim, K. J. *et al.* Inhibition of vascular endothelial growth factor-induced angiogenesis suppresses tumour growth in vivo. *Nature* **362**, 841-844, doi:10.1038/362841a0 (1993).

22 Warren, R. S., Yuan, H., Matli, M. R., Gillett, N. A. & Ferrara, N. Regulation by vascular endothelial growth factor of human colon cancer tumorigenesis in a mouse model of experimental liver metastasis. *J Clin Invest* **95**, 1789-1797, doi:10.1172/JCI117857 (1995).

23 Jain, R. K., Duda, D. G., Clark, J. W. & Loeffler, J. S. Lessons from phase III clinical trials on anti-VEGF therapy for cancer. *Nat Clin Pract Oncol* **3**, 24-40, doi:10.1038/ncponc0403 (2006).

24 Hurwitz, H. *et al.* Bevacizumab plus irinotecan, fluorouracil, and leucovorin for metastatic colorectal cancer. *N Engl J Med* **350**, 2335-2342, doi:10.1056/NEJMoa032691 (2004).

25 Reck, M. *et al.* Phase III trial of cisplatin plus gemcitabine with either placebo or bevacizumab as first-line therapy for nonsquamous non-small-cell lung cancer: AVAil. *J Clin Oncol* **27**, 1227-1234, doi:10.1200/JCO.2007.14.5466 (2009).

26 Saltz, L. B. *et al.* Bevacizumab in combination with oxaliplatin-based chemotherapy as first-line therapy in metastatic colorectal cancer: a randomized phase III study. *J Clin Oncol* **26**, 2013-2019, doi:10.1200/JCO.2007.14.9930 (2008).

27 Sandler, A. *et al.* Paclitaxel-carboplatin alone or with bevacizumab for non-small-cell lung cancer. *N Engl J Med* **355**, 2542-2550, doi:10.1056/NEJMoa061884 (2006).

28 Tebbutt, N. C. *et al.* Capecitabine, bevacizumab, and mitomycin in first-line treatment of metastatic colorectal cancer: results of the Australasian Gastrointestinal Trials Group Randomized Phase III MAX Study. *J Clin Oncol* **28**, 3191-3198, doi:10.1200/JCO.2009.27.7723 (2010).

29 Goel, S. *et al.* Normalization of the vasculature for treatment of cancer and other diseases. *Physiol Rev* **91**, 1071-1121, doi:10.1152/physrev.00038.2010 (2011).

30 Wildiers, H. *et al.* Effect of antivascular endothelial growth factor treatment on the intratumoral uptake of CPT-11. *Br J Cancer* **88**, 1979-1986, doi:10.1038/sj.bjc.6601005 (2003).

31 Yuan, F. *et al.* Time-dependent vascular regression and permeability changes in established human tumor xenografts induced by an anti-vascular endothelial growth factor/vascular permeability factor antibody. *Proc Natl Acad Sci U S A* **93**, 14765-14770 (1996).

32 Batchelor, T. T. *et al.* Phase II study of cediranib, an oral pan-vascular endothelial growth factor receptor tyrosine kinase inhibitor, in patients with recurrent glioblastoma. *J Clin Oncol* **28**, 2817-2823, doi:10.1200/JCO.2009.26.3988 (2010).

33 Willett, C. G. *et al.* Direct evidence that the VEGF-specific antibody bevacizumab has antivascular effects in human rectal cancer. *Nat Med* **10**, 145-147, doi:10.1038/nm988 (2004).

34 Sorensen, A. G. *et al.* A "vascular normalization index" as potential mechanistic biomarker to predict survival after a single dose of cediranib in recurrent glioblastoma patients. *Cancer Res* **69**, 5296-5300, doi:10.1158/0008-5472.CAN-09-0814 (2009).

35 Bottsford-Miller, J. N., Coleman, R. L. & Sood, A. K. Resistance and escape from antiangiogenesis therapy: clinical implications and future strategies. *J Clin Oncol* **30**, 4026-4034, doi:10.1200/JCO.2012.41.9242 (2012).

36 Bergers, G. & Hanahan, D. Modes of resistance to anti-angiogenic therapy. *Nat Rev Cancer* **8**, 592-603, doi:10.1038/nrc2442 (2008).

37 Jain, R. K. Antiangiogenesis strategies revisited: from starving tumors to alleviating hypoxia. *Cancer Cell* **26**, 605-622, doi:10.1016/j.ccell.2014.10.006 (2014).

38 Hillen, F. & Griffioen, A. W. Tumour vascularization: sprouting angiogenesis and beyond. *Cancer Metastasis Rev* **26**, 489-502, doi:10.1007/s10555-007-9094-7 (2007).

39 Krishna Priya, S. *et al.* Tumour angiogenesis-Origin of blood vessels. *Int J Cancer* **139**, 729-735, doi:10.1002/ijc.30067 (2016).

40 Shang, B., Cao, Z. & Zhou, Q. Progress in tumor vascular normalization for anticancer therapy: challenges and perspectives. *Front Med* **6**, 67-78, doi:10.1007/s11684-012-0176-8 (2012).

41 Magrini, E. *et al.* Endothelial deficiency of L1 reduces tumor angiogenesis and promotes vessel normalization. *J Clin Invest* **124**, 4335-4350, doi:10.1172/JCI70683 (2014).

42 Sato, R., Semba, T., Saya, H. & Arima, Y. Stem Cells and Epithelial-Mesenchymal Transition (EMT) in Cancer: Biological Implications and Therapeutic Targets. *Stem Cells*, doi:10.1002/stem.2406 (2016).

43 Reya, T., Morrison, S. J., Clarke, M. F. & Weissman, I. L. Stem cells, cancer, and cancer stem cells. *Nature* **414**, 105-111, doi:10.1038/35102167 (2001).

44 Donnenberg, V. S. & Donnenberg, A. D. Multiple drug resistance in cancer revisited: the cancer stem cell hypothesis. *J Clin Pharmacol* **45**, 872-877, doi:10.1177/0091270005276905 (2005).

45 Bao, S. *et al.* Glioma stem cells promote radioresistance by preferential activation of the DNA damage response. *Nature* **444**, 756-760, doi:10.1038/nature05236 (2006).

46 Wicha, M. S., Liu, S. & Dontu, G. Cancer stem cells: an old idea--a paradigm shift. *Cancer Res* **66**, 1883-1890; discussion 1895-1886, doi:10.1158/0008-5472.CAN-05-3153 (2006).

47 Krishnamurthy, S. *et al.* Endothelial cell-initiated signaling promotes the survival and self-renewal of cancer stem cells. *Cancer Res* **70**, 9969-9978, doi:10.1158/0008-5472.CAN-10-1712 (2010).

48 Calabrese, C. *et al.* A perivascular niche for brain tumor stem cells. *Cancer Cell* **11**, 69-82, doi:10.1016/j.ccr.2006.11.020 (2007).

49 Yang, Z. J. & Wechsler-Reya, R. J. Hit 'em where they live: targeting the cancer stem cell niche. *Cancer Cell* **11**, 3-5, doi:10.1016/j.ccr.2006.12.007 (2007).

50 Lengyel, E. Ovarian cancer development and metastasis. *Am J Pathol* **177**, 1053-1064, doi:10.2353/ajpath.2010.100105 (2010).

51 Shih Ie, M. & Kurman, R. J. Ovarian tumorigenesis: a proposed model based on morphological and molecular genetic analysis. *Am J Pathol* **164**, 1511-1518 (2004).

52 Li, J., Fadare, O., Xiang, L., Kong, B. & Zheng, W. Ovarian serous carcinoma: recent concepts on its origin and carcinogenesis. *J Hematol Oncol* **5**, 8, doi:10.1186/1756-8722-5-8 (2012).

53 Nezhat, F. R., Apostol, R., Nezhat, C. & Pejovic, T. New insights in the pathophysiology of ovarian cancer and implications for screening and prevention. *Am J Obstet Gynecol* **213**, 262-267, doi:10.1016/j.ajog.2015.03.044 (2015).

54 Fathalla, M. F. Incessant ovulation--a factor in ovarian neoplasia? *Lancet* **2**, 163 (1971).

55 Mok, S. C. *et al.* Etiology and pathogenesis of epithelial ovarian cancer. *Dis Markers* **23**, 367-376 (2007).

56 Fleming, J. S., Beaugie, C. R., Haviv, I., Chenevix-Trench, G. & Tan, O. L. Incessant ovulation, inflammation and epithelial ovarian carcinogenesis: revisiting old hypotheses. *Mol Cell Endocrinol* **247**, 4-21, doi:10.1016/j.mce.2005.09.014 (2006).

57 Levanon, K., Crum, C. & Drapkin, R. New insights into the pathogenesis of serous ovarian cancer and its clinical impact. *J Clin Oncol* **26**, 5284-5293, doi:10.1200/JCO.2008.18.1107 (2008).

58 Scully, R. E. Pathology of ovarian cancer precursors. *J Cell Biochem Suppl* **23**, 208-218 (1995).

59 Auersperg, N. Ovarian surface epithelium as a source of ovarian cancers: unwarranted speculation or evidence-based hypothesis? *Gynecol Oncol* **130**, 246-251, doi:10.1016/j.ygyno.2013.03.021 (2013).

60 Crum, C. P. *et al.* The distal fallopian tube: a new model for pelvic serous carcinogenesis. *Curr Opin Obstet Gynecol* **19**, 3-9, doi:10.1097/GCO.0b013e328011a21f (2007).

61 Piek, J. M. *et al.* Dysplastic changes in prophylactically removed Fallopian tubes of women predisposed to developing ovarian cancer. *J Pathol* **195**, 451-456, doi:10.1002/path.1000 (2001).

62 Ng, A. & Barker, N. Ovary and fimbrial stem cells: biology, niche and cancer origins. *Nat Rev Mol Cell Biol* **16**, 625-638, doi:10.1038/nrm4056 (2015).

63 Davidson, B., Trope, C. G. & Reich, R. Epithelial-mesenchymal transition in ovarian carcinoma. *Front Oncol* **2**, 33, doi:10.3389/fonc.2012.00033 (2012).

64 Mani, S. A. *et al.* The epithelial-mesenchymal transition generates cells with properties of stem cells. *Cell* **133**, 704-715, doi:10.1016/j.cell.2008.03.027 (2008).

65 Zeisberg, M. & Neilson, E. G. Biomarkers for epithelial-mesenchymal transitions. *J Clin Invest* **119**, 1429-1437, doi:10.1172/JCI36183 (2009).

66 Takai, M. *et al.* The EMT (epithelial-mesenchymal-transition)-related protein expression indicates the metastatic status and prognosis in patients with ovarian cancer. *J Ovarian Res* **7**, 76, doi:10.1186/1757-2215-7-76 (2014).

67 Kajiyama, H. *et al.* Chemoresistance to paclitaxel induces epithelial-mesenchymal transition and enhances metastatic potential for epithelial ovarian carcinoma cells. *Int J Oncol* **31**, 277-283 (2007).

68 Rohnalter, V. *et al.* A multi-stage process including transient polyploidization and EMT precedes the emergence of chemoresistent ovarian carcinoma cells with a dedifferentiated and pro-inflammatory secretory phenotype. *Oncotarget* **6**, 40005-40025, doi:10.18632/oncotarget.5552 (2015).

69 Davidson, B. *et al.* The clinical role of epithelial-mesenchymal transition and stem cell markers in advanced-stage ovarian serous carcinoma effusions. *Hum Pathol* **46**, 1-8, doi:10.1016/j.humpath.2014.10.004 (2015).

70 Baba, T. *et al.* Epigenetic regulation of CD133 and tumorigenicity of CD133+ ovarian cancer cells. *Oncogene* **28**, 209-218, doi:10.1038/onc.2008.374 (2009).

71 Curley, M. D. *et al.* CD133 expression defines a tumor initiating cell population in primary human ovarian cancer. *Stem Cells* **27**, 2875-2883, doi:10.1002/stem.236 (2009).

72 Landen, C. N., Jr. *et al.* Targeting aldehyde dehydrogenase cancer stem cells in ovarian cancer. *Mol Cancer Ther* **9**, 3186-3199, doi:10.1158/1535-7163.MCT-10-0563 (2010).

73 Zhang, S. *et al.* Identification and characterization of ovarian cancer-initiating cells from primary human tumors. *Cancer Res* **68**, 4311-4320, doi:10.1158/0008-5472.CAN-08-0364 (2008).

74 Zhang, J. *et al.* CD133 expression associated with poor prognosis in ovarian cancer. *Mod Pathol* **25**, 456-464, doi:10.1038/modpathol.2011.170 (2012).

75 Kusumbe, A. P., Mali, A. M. & Bapat, S. A. CD133-expressing stem cells associated with ovarian metastases establish an endothelial hierarchy and contribute to tumor vasculature. *Stem Cells* **27**, 498-508, doi:10.1634/stemcells.2008-0868 (2009).

76 Silva, I. A. *et al.* Aldehyde dehydrogenase in combination with CD133 defines angiogenic ovarian cancer stem cells that portend poor patient survival. *Cancer Res* **71**, 3991-4001, doi:10.1158/0008-5472.CAN-10-3175 (2011).

77 Mitamura, T., Gourley, C. & Sood, A. K. Prediction of anti-angiogenesis escape. *Gynecol Oncol* **141**, 80-85, doi:10.1016/j.ygyno.2015.12.033 (2016).

78 Sahade, M., Caparelli, F. & Hoff, P. M. Cediranib: a VEGF receptor tyrosine kinase inhibitor. *Future Oncol* **8**, 775-781, doi:10.2217/fon.12.73 (2012).

79 du Bois, A. *et al.* Incorporation of pazopanib in maintenance therapy of ovarian cancer. *J Clin Oncol* **32**, 3374-3382, doi:10.1200/JCO.2014.55.7348 (2014).

80 Byrne, A. T. *et al.* Vascular endothelial growth factor-trap decreases tumor burden, inhibits ascites, and causes dramatic vascular remodeling in an ovarian cancer model. *Clin Cancer Res* **9**, 5721-5728 (2003).

81 Adam, R. A. & Adam, Y. G. Malignant ascites: past, present, and future. *J Am Coll Surg* **198**, 999-1011, doi:10.1016/j.jamcollsurg.2004.01.035 (2004).

82 Ahmed, N. & Stenvers, K. L. Getting to know ovarian cancer ascites: opportunities for targeted therapy-based translational research. *Front Oncol* **3**, 256, doi:10.3389/fonc.2013.00256 (2013).

83 Bellati, F. *et al.* Complete remission of ovarian cancer induced intractable malignant ascites with intraperitoneal bevacizumab. Immunological observations and a literature review. *Invest New Drugs* **28**, 887-894, doi:10.1007/s10637-009-9351-4 (2010).

84 Numnum, T. M., Rocconi, R. P., Whitworth, J. & Barnes, M. N. The use of bevacizumab to palliate symptomatic ascites in patients with refractory ovarian carcinoma. *Gynecol Oncol* **102**, 425-428, doi:10.1016/j.ygyno.2006.05.018 (2006).

85 Colombo, N. *et al.* A phase II study of aflibercept in patients with advanced epithelial ovarian cancer and symptomatic malignant ascites. *Gynecol Oncol* **125**, 42-47, doi:10.1016/j.ygyno.2011.11.021 (2012).

86 Kipps, E., Tan, D. S. & Kaye, S. B. Meeting the challenge of ascites in ovarian cancer: new avenues for therapy and research. *Nat Rev Cancer* **13**, 273-282, doi:10.1038/nrc3432 (2013).

87 Smolle, E., Taucher, V. & Haybaeck, J. Malignant ascites in ovarian cancer and the role of targeted therapeutics. *Anticancer Res* **34**, 1553-1561 (2014).

88 Yang, X., Shen, F., Hu, W., Coleman, R. L. & Sood, A. K. New ways to successfully target tumor vasculature in ovarian cancer. *Curr Opin Obstet Gynecol* **27**, 58-65, doi:10.1097/GCO.0000000000000136 (2015).

89 Moos, M. *et al.* Neural adhesion molecule L1 as a member of the immunoglobulin superfamily with binding domains similar to fibronectin. *Nature* **334**, 701-703, doi:10.1038/334701a0 (1988).

90 Maness, P. F. & Schachner, M. Neural recognition molecules of the immunoglobulin superfamily: signaling transducers of axon guidance and neuronal migration. *Nat Neurosci* **10**, 19-26, doi:10.1038/nn1827 (2007).

91 Wei, C. H. & Ryu, S. E. Homophilic interaction of the L1 family of cell adhesion molecules. *Exp Mol Med* **44**, 413-423, doi:10.3858/emm.2012.44.7.050 (2012).

92 Beer, S., Oleszewski, M., Gutwein, P., Geiger, C. & Altevogt, P. Metalloproteinase-mediated release of the ectodomain of L1 adhesion molecule. *J Cell Sci* **112 (Pt 16)**, 2667-2675 (1999).

93 Fogel, M. *et al.* L1 expression as a predictor of progression and survival in patients with uterine and ovarian carcinomas. *Lancet* **362**, 869-875, doi:10.1016/S0140-6736(03)14342-5 (2003).

94 Mechtersheimer, S. *et al.* Ectodomain shedding of L1 adhesion molecule promotes cell migration by autocrine binding to integrins. *J Cell Biol* **155**, 661-673, doi:10.1083/jcb.200101099 (2001).

95 Stoeck, A. *et al.* L1-CAM in a membrane-bound or soluble form augments protection from apoptosis in ovarian carcinoma cells. *Gynecol Oncol* **104**, 461-469, doi:10.1016/j.ygyno.2006.08.038 (2007).

96 Friedli, A. *et al.* The soluble form of the cancer-associated L1 cell adhesion molecule is a pro-angiogenic factor. *Int J Biochem Cell Biol* **41**, 1572-1580, doi:10.1016/j.biocel.2009.01.006 (2009).

97 Kiefel, H. *et al.* L1CAM: a major driver for tumor cell invasion and motility. *Cell Adh Migr* **6**, 374-384, doi:10.4161/cam.20832 (2012).

98 Cavallaro, U. & Dejana, E. Adhesion molecule signalling: not always a sticky business. *Nat Rev Mol Cell Biol* **12**, 189-197, doi:10.1038/nrm3068 (2011).

99 Rathjen, F. G. & Schachner, M. Immunocytological and biochemical characterization of a new neuronal cell surface component (L1 antigen) which is involved in cell adhesion. *Embo J* **3**, 1-10 (1984).

100 Maddaluno, L. *et al.* The adhesion molecule L1 regulates transendothelial migration and trafficking of dendritic cells. *J Exp Med* **206**, 623-635, doi:jem.20081211 [pii]10.1084/jem.20081211 (2009).

101 Raveh, S., Gavert, N. & Ben-Ze'ev, A. L1 cell adhesion molecule (L1CAM) in invasive tumors. *Cancer Lett* **282**, 137-145, doi:10.1016/j.canlet.2008.12.021 (2009).

102 Bondong, S. *et al.* Prognostic significance of L1CAM in ovarian cancer and its role in constitutive NF-kappaB activation. *Ann Oncol* **23**, 1795-1802, doi:10.1093/annonc/mdr568 (2012).

103 Gast, D. *et al.* L1 augments cell migration and tumor growth but not beta3 integrin expression in ovarian carcinomas. *Int J Cancer* **115**, 658-665, doi:10.1002/ijc.20869 (2005).

104 Zecchini, S. *et al.* The differential role of L1 in ovarian carcinoma and normal ovarian surface epithelium. *Cancer Res* **68**, 1110-1118 (2008).

105 Arlt, M. J. *et al.* Efficient inhibition of intra-peritoneal tumor growth and dissemination of human ovarian carcinoma cells in nude mice by anti-L1-cell adhesion molecule monoclonal antibody treatment. *Cancer Res* **66**, 936-943, doi:10.1158/0008-5472.CAN-05-1818 (2006).

106 Wolterink, S. *et al.* Therapeutic antibodies to human L1CAM: functional characterization and application in a mouse model for ovarian carcinoma. *Cancer Res* **70**, 2504-2515, doi:10.1158/0008-5472.CAN-09-3730 (2010).

107 Schafer, H. *et al.* Combined treatment of L1CAM antibodies and cytostatic drugs improve the therapeutic response of pancreatic and ovarian carcinoma. *Cancer Lett* **319**, 66-82, doi:10.1016/j.canlet.2011.12.035 (2012).

108 Issa, Y. *et al.* Enhanced L1CAM expression on pancreatic tumor endothelium mediates selective tumor cell transmigration. *J Mol Med (Berl)* **87**, 99-112, doi:10.1007/s00109-008-0410-7 (2009).

109 Garlanda, C. *et al.* Progressive growth in immunodeficient mice and host cell recruitment by mouse endothelial cells transformed by polyoma middle-sized T antigen: implications for the pathogenesis of opportunistic vascular tumors. *Proc Natl Acad Sci U S A* **91**, 7291-7295 (1994).

110 Greenaway, J., Moorehead, R., Shaw, P. & Petrik, J. Epithelial-stromal interaction increases cell proliferation, survival and tumorigenicity in a mouse model of human epithelial ovarian cancer. *Gynecol Oncol* **108**, 385-394, doi:10.1016/j.ygyno.2007.10.035 (2008).

111 Kisanuki, Y. Y. *et al.* Tie2-Cre transgenic mice: a new model for endothelial cell-lineage analysis in vivo. *Dev Biol* **230**, 230-242, doi:10.1006/dbio.2000.0106 (2001).

112 Law, J. W. *et al.* Decreased anxiety, altered place learning, and increased CA1 basal excitatory synaptic transmission in mice with conditional ablation of the neural cell adhesion molecule L1. *J Neurosci* **23**, 10419-10432 (2003).

113 Bamias, A., Pignata, S. & Pujade-Lauraine, E. Angiogenesis: a promising therapeutic target for ovarian cancer. *Crit Rev Oncol Hematol* **84**, 314-326, doi:10.1016/j.critrevonc.2012.04.002 (2012).

114 Cho, S. *et al.* Characterization and evaluation of pre-clinical suitability of a syngeneic orthotopic mouse ovarian cancer model. *Anticancer Res* **33**, 1317-1324 (2013).

115 Lieu, C., Heymach, J., Overman, M., Tran, H. & Kopetz, S. Beyond VEGF: inhibition of the fibroblast growth factor pathway and antiangiogenesis. *Clin Cancer Res* **17**, 6130-6139, doi:10.1158/1078-0432.CCR-11-0659 (2011).

116 Presta, M. *et al.* Fibroblast growth factor/fibroblast growth factor receptor system in angiogenesis. *Cytokine Growth Factor Rev* **16**, 159-178, doi:10.1016/j.cytogfr.2005.01.004 (2005).

117 Mohammadi, M. *et al.* Crystal structure of an angiogenesis inhibitor bound to the FGF receptor tyrosine kinase domain. *Embo J* **17**, 5896-5904, doi:10.1093/emboj/17.20.5896 (1998).

118 Yadav, S. S. & Narayan, G. Role of ROBO4 signalling in developmental and pathological angiogenesis. *Biomed Res Int* **2014**, 683025, doi:10.1155/2014/683025 (2014).

119 Koch, A. W. *et al.* Robo4 maintains vessel integrity and inhibits angiogenesis by interacting with UNC5B. *Dev Cell* **20**, 33-46, doi:10.1016/j.devcel.2010.12.001 (2011).

120 Fahmy, R. G., Dass, C. R., Sun, L. Q., Chesterman, C. N. & Khachigian, L. M. Transcription factor Egr-1 supports FGF-dependent angiogenesis during neovascularization and tumor growth. *Nat Med* **9**, 1026-1032, doi:10.1038/nm905 (2003).

121 Lucerna, M. *et al.* Sustained expression of early growth response protein-1 blocks angiogenesis and tumor growth. *Cancer Res* **66**, 6708-6713, doi:10.1158/0008-5472.CAN-05-2732 (2006).

122 Bhowmick, N. A., Neilson, E. G. & Moses, H. L. Stromal fibroblasts in cancer initiation and progression. *Nature* **432**, 332-337, doi:10.1038/nature03096 (2004).

123 Orimo, A. *et al.* Stromal fibroblasts present in invasive human breast carcinomas promote tumor growth and angiogenesis through elevated SDF-1/CXCL12 secretion. *Cell* **121**, 335-348, doi:10.1016/j.cell.2005.02.034 (2005).

124 Zeng, Q. *et al.* Crosstalk between tumor and endothelial cells promotes tumor angiogenesis by MAPK activation of Notch signaling. *Cancer Cell* **8**, 13-23, doi:10.1016/j.ccr.2005.06.004 (2005).

125 Kaneko, T. *et al.* Bcl-2 orchestrates a cross-talk between endothelial and tumor cells that promotes tumor growth. *Cancer Res* **67**, 9685-9693, doi:10.1158/0008-5472.CAN-07-1497 (2007).

126 Zhang, L. *et al.* Generation of a syngeneic mouse model to study the effects of vascular endothelial growth factor in ovarian carcinoma. *Am J Pathol* **161**, 2295-2309 (2002).

127 Janat-Amsbury, M. M., Yockman, J. W., Anderson, M. L., Kieback, D. G. & Kim, S. W. Comparison of ID8 MOSE and VEGF-modified ID8 cell lines in an immunocompetent animal model for human ovarian cancer. *Anticancer Res* **26**, 2785-2789 (2006).

128 Tsai, J. H. & Yang, J. Epithelial-mesenchymal plasticity in carcinoma metastasis. *Genes Dev* **27**, 2192-2206, doi:10.1101/gad.225334.113 (2013).

129 Pietila, M., Ivaska, J. & Mani, S. A. Whom to blame for metastasis, the epithelial-mesenchymal transition or the tumor microenvironment? *Cancer Lett* **380**, 359-368, doi:10.1016/j.canlet.2015.12.033 (2016).

130 Topcul, M. & Cetin, I. Clinical significance of epithelial-mesenchymal transition and cancer stem cells. *J Buon* **21**, 312-319 (2016).

131 Lee, C. H., Yu, C. C., Wang, B. Y. & Chang, W. W. Tumorsphere as an effective in vitro platform for screening anti-cancer stem cell drugs. *Oncotarget* **7**, 1215-1226, doi:10.18632/oncotarget.6261 (2016).

132 Sansone, P. *et al.* IL-6 triggers malignant features in mammospheres from human ductal breast carcinoma and normal mammary gland. *J Clin Invest* **117**, 3988-4002, doi:10.1172/JCI32533 (2007).

133 Wang, H. *et al.* Targeting interleukin 6 signaling suppresses glioma stem cell survival and tumor growth. *Stem Cells* **27**, 2393-2404, doi:10.1002/stem.188 (2009).

134 Fuso Nerini, I., Cesca, M., Bizzaro, F. & Giavazzi, R. Combination therapy in cancer: effects of angiogenesis inhibitors on drug pharmacokinetics and pharmacodynamics. *Chin J Cancer* **35**, 61, doi:10.1186/s40880-016-0123-1 (2016).

135 Dickson, P. V. *et al.* Bevacizumab-induced transient remodeling of the vasculature in neuroblastoma xenografts results in improved delivery and efficacy of systemically administered chemotherapy. *Clin Cancer Res* **13**, 3942-3950, doi:10.1158/1078-0432.CCR-07-0278 (2007).

136 Turley, R. S. *et al.* Bevacizumab-induced alterations in vascular permeability and drug delivery: a novel approach to augment regional chemotherapy for in-transit melanoma. *Clin Cancer Res* **18**, 3328-3339, doi:10.1158/1078-0432.CCR-11-3000 (2012).

137 Cesca, M. *et al.* Bevacizumab-Induced Inhibition of Angiogenesis Promotes a More Homogeneous Intratumoral Distribution of Paclitaxel, Improving the Antitumor Response. *Mol Cancer Ther* **15**, 125-135, doi:10.1158/1535-7163.MCT-15-0063 (2016).

138 Cesca, M. *et al.* The effects of vandetanib on paclitaxel tumor distribution and antitumor activity in a xenograft model of human ovarian carcinoma. *Neoplasia* **11**, 1155-1164 (2009).

139 Doherty, P. & Walsh, F. S. CAM-FGF receptor interactions: a model for axonal growth. *Mol Cell Neurosci* **8**, 99-111, doi:10.1006/mcne.1996.0049 (1996).

140 Kulahin, N. *et al.* Fibronectin type III (FN3) modules of the neuronal cell adhesion molecule L1 interact directly with the fibroblast growth factor (FGF) receptor. *Mol Cell Neurosci* **37**, 528-536, doi:10.1016/j.mcn.2007.12.001 (2008).

141 Mohanan, V., Temburni, M. K., Kappes, J. C. & Galileo, D. S. L1CAM stimulates glioma cell motility and proliferation through the fibroblast growth factor receptor. *Clin Exp Metastasis* **30**, 507-520, doi:10.1007/s10585-012-9555-4 (2013).

142 Francavilla, C. *et al.* The binding of NCAM to FGFR1 induces a specific cellular response mediated by receptor trafficking. *J Cell Biol* **187**, 1101-1116, doi:10.1083/jcb.200903030 (2009).

143 Francavilla, C. *et al.* Neural cell adhesion molecule regulates the cellular response to fibroblast growth factor. *J Cell Sci* **120**, 4388-4394, doi:10.1242/jcs.010744 (2007).

144 Daniele, G., Corral, J., Molife, L. R. & de Bono, J. S. FGF receptor inhibitors: role in cancer therapy. *Curr Oncol Rep* **14**, 111-119, doi:10.1007/s11912-012-0225-0 (2012).

145 Huszar, M. *et al.* Up-regulation of L1CAM is linked to loss of hormone receptors and E-cadherin in aggressive subtypes of endometrial carcinomas. *J Pathol* **220**, 551-561, doi:10.1002/path.2673 (2010).

146 Shtutman, M., Levina, E., Ohouo, P., Baig, M. & Roninson, I. B. Cell adhesion molecule L1 disrupts E-cadherin-containing adherens junctions and increases scattering and motility of MCF7 breast carcinoma cells. *Cancer Res* **66**, 11370-11380, doi:10.1158/0008-5472.CAN-06-2106 (2006).

ACKNOWLEDGMENTS

I thank my Supervisor Ugo Cavallaro for the opportunity to work in his lab and the support he gave me during my PhD.

I thank Fabrizio Bianchi for his help with bioinformatic and statistical analyses.

I thank Giovanni Bertalot for his precious help with immunohistochemical analysis.

I thank my internal supervisor Elisabetta Dejana and my external supervisor Gerhard Christofori for their useful suggestions and their support.

I thank Elena Magrini for her helps and useful discussions.

I also thank Pier Paolo Di Fiore for his support.

I especially thank everyone who helped me during these years at IEO, including all the Facilities and the SEMM office.

Con la forma ora basta,
è il momento di mettere le mani in pasta.
Non sono brava con le smancerie
ma il mio GRAZIE deve arrivare fino alle periferie.

Tocca al primo della lista
visto che è lui che mi ha lanciato in questa pista.
Siamo alla fine e si può dire,
ce ne fossero di capi come lui a non finire.
Sempre presente e pieno di sapere

non esiste cosa che non riesca a prevedere.
Su qualcosa è un po' intransigente:
manca sempre un controllo, quello più pertinente.
E te che ti eri impegnata,
fai la fine della neo-laureata
e ti chiedi come mai
quello giusto non lo becchi mai!
Un altro puntiglio va svelato,
ecco l'errore che non avevi rivelato:
dopo attente letture e riletture
ti sei illusa che non ci fossero brutture.
Ma lui, basta che apra il primo foglio
ed individua un bell'imbroglio.
Cerchi svelta la giustificazione,
ma poi capisci che sarà il primo di una serie
e ti arrendi alle tue miserie.
A parte questo non ci si può lamentare
e non posso fare altro che ringraziare,
tante cose mi hai insegnato,
e a questo mondo mi hai appassionato.

Ora tocca alle colleghe,
ormai sono amiche e quelle vere.
Tocca ora alla Lupiaaaaa,
e meno male che il vento non me la ha mai portata via.
Quando da Milano me ne andrò,
qualche sassolino in tasca ti metterò
così anche i miei successori,
potranno godere di tutti i tuoi consigli migliori.

Dovete sapere che delle cellule è la regina,
le passerebbe dalla sera alla mattina.
Per i western invece vi conviene andare altrove
a meno che non vi divertiate a fare molte prove.
Sembra un tipo solitario ma nonostante le sue intenzioni,
non mi sono MAI arresa alle sue poche interazioni.
Ti ho capito cara bella, niente baci e coccoline
ma alla fine mi vuoi bene quasi come alle tue nipotine.

Ecco ora Ale Willa,
sempre a ridere e sempre arzilla.
Nonostante la tua dipartita
hai sempre un posto di rilievo nella mia vita.
Abbiamo iniziato con fagi e purificazioni
e poi un cambio di intenzioni
sepolte tra pancreas e topolini
ci siamo divertite come due cittini.
E anche se tra i crucchi sei finita
resteremo sempre e solo NOI le tue colleghe
e per tutta la vita!

Qualche rima anche per il nuovo arrivato,
da Cosenza si è palesato.
Sei stato un bel sostegno
soprattutto nella stesura della tesi, che è un bell'impegno!
La mia mancanza anche dopo il PhD non sentirai,
con me e lupis tutti i santi imparerai.
Per non parlare del toscano,
non ci telefonerai più al ristorante

ma lo chiamerai come una persona importante.

Alla fine a tutti gli altri un grande grazie,

perché avete condiviso le mie gioie e le mie disgrazie!

Grazie a GB che ha l'occhio brevettato

e in letture e colorazioni è specializzato.

Sono indietro di qualche ricciarello,

ma rimedierò e magari anche con il brunello.

Grazie a Fabri per le analisi,

senza di te la statistica mi avrebbe fatto venire una paralisi.

Sul disordine mi puoi ancora rimproverare,

perché ho sempre tanto da imparare.

Grazie a Ste e MIC per il vostro buon umore

e per essere disponibili anche per me a tutte lo ore.

Grazie Stefinco per il tuo aiuto costante,

sei una garanzia e un amico strabiliate.

Grazie anche Stefina e a Rosmarina,

garantiscono risate dalla sera alla mattina.

Grazie anche a tutti gli altri,

non vi nomino e non è maleducazione

ma per evitare che i ringraziamenti diventino un sermone.